

"AUREL VLAICU" UNIVERSITY OF ARAD
FACULTY OF FOOD ENGINEERING, TOURISM AND ENVIRONMENTAL PROTECTION
CHEMICAL AND TECHNOLOGICAL RESEARCH CENTER

Scientific and Technical Bulletin

Series CHEMISTRY, FOOD SCIENCE & ENGINEERING



**PECTIN QUANTIFICATION FROM CELLULOSIC/LIGNOCELLULOSIC RAW
MATERIALS BY FT-IR ATR ANALYSIS (pages 20-25)**

Year XVIII, Vol. 17, 2020

ISSN 1582-1021

e-ISSN 2668-4764

“AUREL VLAICU” UNIVERSITY OF ARAD
FACULTY OF FOOD ENGINEERING, TOURISM AND ENVIRONMENTAL
PROTECTION
CHEMICAL AND TECHNOLOGICAL RESEARCH CENTER

Scientific and Technical Bulletin

Series CHEMISTRY, FOOD SCIENCE & ENGINEERING

Year XVIII, Vol. 17, 2020

ISSN 1582-1021

e-ISSN 2668-4764



EDITURA UNIVERSITĂȚII
AUREL VLAICU



A R A D

CONTENTS

- 3** DYNAMICS OF ANTIOXIDANT CHARACTER OF EXTRACTS FROM FLAX SEEDS UNDER VARIABLE CONDITIONS
Andreea LUPITU, Nicolae DINCA
- 9** STUDENTS KNOWLEDGE ASSESSMENT CRITERIA
Simona GAVRILAȘ
- 15** HIGH RESOLUTION MASS SPECTROMETRY WITH CHIP-BASED IONIZATION FOR THE ASSESSMENT OF NONCOVALENT INTERACTIONS OF PROTEINS WITH NORMAL BRAIN AND BRAIN TUMOR GANGLIOSIDES
Raluca ICĂ, Mirela SÂRBU, Alina D. ZAMFIR
- 20** PECTIN QUANTIFICATION FROM CELLULOSIC/LIGNOCELLULOSIC RAW MATERIALS BY FT-IR ATR ANALYSIS
Dorina Rodica CHAMBRE, Mihaela DOCHIA
- 26** THE INFLUENCE OF AIR POLLUTANTS ON DIFFERENT MATERIAL USED IN CONSTRUCTION OF MONUMENTS
Alexandru BOGDAN, Lucian COPOLOVICI
- 29** THE INFLUENCE OF GRAPEVINE PRUNING ON THE LEVEL CROP AND AND QUALITY IN CABERNET SAUVIGNON CLONES
Constantin BADUCA, Felicia STOICA, Camelia MUNTEAN
- 33** ZR(IV) MOFS BASED ON TEREPHTHALIC ACID AND ACETIC ACID MODULATOR
Mirela PICIORUS, Alexandru POPA, Catalin IANASI, Elisabeta I. SZERB, Carmen CRETU
- 42** INDUCTION OF LIQUID CRYSTALLINE PROPERTIES IN PT(II) COORDINATION COMPLEXES BASED ON TERPYRIDINE AND GALLATE LIGANDS
Evelyn POPA1, Elisabeta I. SZERB1, Adelina-Antonia ANDELESCU1
- 49** SCIENTIFIC EVENT: STUDENT SCIENTIFIC SESSION AT FACULTY OF FOOD ENGINEERING, TOURISM AND ENVIRONMENTAL PROTECTION, 2020
Dana Maria COPOLOVICI

EDITORIAL BOARD

Dana M. COPOLOVICI, Editor-in-chief

„Aurel Vlaicu” University of Arad, Romania

EDITORS

Dorina CHAMBREE, „Aurel Vlaicu” University of Arad, Romania

Lucian COPOLOVICI, „Aurel Vlaicu” University of Arad, Romania

Calina Petruta CORNEA, University of Agricultural Sciences and Veterinary Medicine
Bucharest, Romania

Nicolae DINCĂ, „Aurel Vlaicu” University of Arad, Romania

Simona GAVRILAȘ, „Aurel Vlaicu” University of Arad, Romania

Florentina MUNTEANU, „Aurel Vlaicu” University of Arad, Romania

Mariana-Atena POIANA, Banat’s University of Agricultural Sciences and Veterinary Medicine
“King Mihai I of Romania” from Timisoara, Romania

Ionel POPESCU-MITROI, „Aurel Vlaicu” University of Arad, Romania

Diana RABA, Banat’s University of Agricultural Sciences and Veterinary Medicine “King Mihai I
of Romania” from Timisoara, Romania

Dana RADU, „Aurel Vlaicu” University of Arad, Romania

Loredana SORAN, National Institute for Research & Development of Isotopic and Molecular
Technologies, Cluj-Napoca, Romania

Elisabeta Ildiko SZERB, Institute of Chemistry Timisoara of Romanian Academy

Radu ȘUMALAN, Banat’s University of Agricultural Sciences and Veterinary Medicine “King
Mihai I of Romania” from Timisoara, Romania

Renata ȘUMALAN, Banat’s University of Agricultural Sciences and Veterinary Medicine “King
Mihai I of Romania” from Timisoara, Romania

Simona VICAȘ, University of Oradea, Romania

Irina VOLF, „Gheorghe Asachi” Technical University of Iasi, Romania

Alina D. ZAMFIR, „Aurel Vlaicu” University of Arad, Romania

Cristian MOISA, „Aurel Vlaicu” University of Arad, Romania

COVER DESIGN

Dana Copolovici, "Aurel Vlaicu" University of Arad, Romania






ADDRESS

Faculty of Food Engineering, Tourism and Environmental Protection,
„Aurel Vlaicu” University, Elena Dragoi St., Nr. 2, L31, Arad, Romania

Phone: 0040257369091

E-mail: dana.copolovici@uav.ro

Scientific and Technical Bulletin, Series: Chemistry, Food Science and Engineering is covered/indexed/abstracted in:

	Directory of Research Journals Indexing
	Directory of Open Access Scholarly Resources
	World Cat
	Google Scholar
	CABI

DYNAMICS OF ANTIOXIDANT CHARACTER OF EXTRACTS FROM FLAX SEEDS UNDER VARIABLE CONDITIONS

Andreea LUPITU^{1,2}, Nicolae DINCA^{1*}

¹Faculty of Food Engineering, Tourism and Environmental Protection, "Aurel Vlaicu" University, Romania, 2 Elena Dragoi, Arad 310330, Romania

²Research Development Innovation in Natural and Technical Sciences Institute, "Aurel Vlaicu" University, Romania, 2 Elena Dragoi, Arad 310330, Romania

*Corresponding author email: nicolae.dinca@uav.ro

Abstract: The antioxidant character of natural extracts is an important indicator of quality. In extracts from flax seeds, this character is due to a series of biologically active natural compounds. Our experimental design studies the dynamics of antioxidant character due to the variation of three independent variables at two and three levels: solvent composition (ethanol/water 60:40, 80:20, and 100:0 v/v) extraction time (2, 3, and 4 h), and hydrolysis temperature (60 and 80°C). The antioxidant character (dependent variable) of extracts was expressed in the percentage of DPPH inhibition. The polynomial equation obtained by multiple regression analysis indicates that the influence of the three factors on the studied intervals decreases in order: solvent ratio ethanol > extraction time > hydrolysis temperature. In the studied intervals of the variables, the antioxidant character varies between 40.8 - 75.9 % DPPH inhibition. Response surface graphics and calculated nomograms show how much temperature and time can be reduced in the process without the antioxidant character being substantially affected. The experimental design and data processing described herein may constitute a management model of an optimal industrial extraction process from flax seeds.

Keywords: antioxidant character, flax seeds, multiple regression analysis, extraction optimization.

INTRODUCTION

Antioxidants may be defined as substances that inhibit oxidation. Antioxidants are produced naturally by the biological system and occur in many foods. In plants, via the shikimic acid pathway, phenolic and polyphenolic compounds are produced, which have antioxidant character.

In food products, antioxidants are deliberately added to delay lipid oxidation during processing and storage. They have unique properties of extending the shelf-life of food products without changing their sensory or nutritional qualities. (Shahidi and Ambigaipalan, 2015)

1, 1 - diphenyl - 2 - picrylhydrazyl (DPPH) free radical scavenging method evaluates the antioxidant character of a compound, an extract, or other biological sources. The DPPH method is rapid, simple, inexpensive, and widely used to measure the antioxidant character of foods and/or food products. (Kedare and Singh, 2011) This method has been utilized for investigating the antioxidant character of wheat grain, and bran, vegetables, herbs, edible seed oils, and flours in several different solvent systems including ethanol, aqueous acetone, methanol,

aqueous alcohol, and benzene (Parry et al., 2005). It is a convenient method for the antioxidant assay of cysteine, glutathione, ascorbic acid, tocopherol, and polyhydroxy aromatic compounds (Nishizawa et al., 2005), for olive oil, fruits, juices, and wines (Sánchez-Moreno, 2002).

The determination of the antioxidant character of various types of samples using DPPH is comparable to other methods. (Kedare and Singh, 2011)

The purpose of our work was to study the effect of solvent composition, extraction time, and hydrolysis temperature over the dynamics of the antioxidant character of extracts obtained from flax seeds using a three-level experimental model.

MATERIALS AND METHODS

Extraction of phenolic compounds

Based on the previously reported extraction conditions (Chen et al., 2007; Lupitu and Dinca, 2019; Popova et al., 2009; Willfor et al., 2006), an design with 18 experiments was created to

find the level of antioxidant character depending on the extraction conditions. In order to obtain the crude extracts, 15 g portions of flax seed (Cosmin variety), milled, dried and defatted were extracted for 2, 3 and 4 hours at 60°C, using three proportion of ethanol/water: 60:40, 80:20 and 100:0 v/v (Table 1). The obtained extracts were hydrolysed for 2 hours using hydrochloric acid at 60 and 80°C, and then neutralized and filtered.

Reagents, solvents, and standards

Reagents and solvents used in the experiments were of adequate analytical grade and were obtained from Sigma Aldrich (Fluka, Switzerland), Merck (Darmstadt, Germany) and Chimreactiv (Romania).

Measurement of antioxidant character

The antioxidant character of the extracts was assessed using the DPPH method. Briefly, 3 mL of 0.2 mM DPPH in ethanol were mixed with 0.1 mL sample. This mixture was kept in the dark for 60 minutes. The absorbance was measured against a control sample, at 517 nm using a Specord 200 UV-VIS double-beam spectrophotometer (Analytik Jena Inc. Germany). The calculation of DPPH free radical inhibition, I (%), was performed according to the relation displayed in equation 1:

$$I(\%) = \frac{Abs_{control} - Abs_{sample}}{Abs_{control}} \times 100 \quad (1)$$

where: $Abs_{control}$ represents the absorbance of the control sample consisted of 0.2 mM DPPH in ethanol and Abs_{sample} represents the absorbance of 0.2 mM DPPH containing the investigated extract. All analyzes were performed in triplicate and the results were reported as mean \pm SD. (Metzner Ungureanu et al., 2020)

Experimental design

An experimental design, with three variables X_1 (solvent composition), X_2 (extraction time) and X_3 (hydrolysis temperature), at two and three variation levels (Table 1), was used to study the effect in the extraction process. The corresponding encodings are symbolized x_1 , x_2 and x_3 (Myers & Montgomery, 2002).

Table 1 Independent variable values of the process, the corresponding levels, and their codification

Independent variable	Level			
	x_i	-1	0	1
Solvent composition (ethanol: water, v/v)	X_1	60:40	80:20	100:0
Extraction time (h)	X_2	2	3	4
Hydrolysis temperature (°C)	X_3	60	-	80

Data analysis

The multiple regression procedure and analysis of variance (ANOVA) from MS Excel 2019 software were used (Home Page of Excel 2019). The codified and experimental data (Table 2) were fitted to a polynomial model and regression coefficients were obtained. The generalized polynomial model used for establishing the importance and interaction of the studied factors was as follows:

$$Y_i = \beta_0 + \beta_1 x_1 + \beta_2 x_2 + \beta_3 x_3 + \beta_{12} x_1 x_2 + \beta_{13} x_1 x_3 + \beta_{23} x_2 x_3 + \beta_{11} x_1^2 + \beta_{22} x_2^2 + \beta_{33} x_3^2 + \beta_{123} x_1 x_2 x_3 \quad (2)$$

where Y_i is predicted response, β_0 is intercept, β_1 , β_2 , β_3 , β_{11} , β_{22} and β_{33} is linear and quadratic effect terms, and β_{12} , β_{13} , β_{23} and β_{123} are interaction effects.

RESULTS AND DISCUSSIONS

Fitting the model

The multiple regression equation obtained with MS Excel 2019 is an empirical relationship between antioxidant character (% DPPH inhibition) and the three factors in coded units. The significance of each coefficient was appreciated using the *Student t* test and *p-value* calculated at 95% confidence interval. The corresponding variables will be more significant if the absolute *t* value is larger or the *p-value* is smaller (Home Page of NIST/SEMATECH, 2013). Consequently, the significance of the factors decreases in the order $x_1 > x_2 > x_3$ and the interaction between them in the order $x_1 x_2 > x_1 x_3 \approx x_1 x_2 x_3 > x_2 x_3$ (Table 3). The minus sign of the coefficient indicates an inverse action of factor on the antioxidant character. The action of

the factor is stronger if the absolute value of its coefficient is greater. The high negative value of β_{11} shows that after the maximum, the decrease of the oxidizing character is abrupt with the increase of the ethanol concentration in the extraction solvent (Figures 1 and 2).

Table 2. The experimental design with three variables, the observed responses, and predicted values for antioxidant character, % inhibition of DPPH

Treat	Variable levels			Experimental Y_i	Predicted Y_i
	x_1	x_2	x_3		
1	-1	-1	-1	36.20	32.43
2	0	-1	-1	29.18	36.80
3	1	-1	-1	-3.36	-6.73
4	-1	0	-1	50.56	50.36
5	0	0	-1	41.3	42.46
6	1	0	-1	-12.35	-13.34
7	-1	1	-1	62.42	68.29
8	0	1	-1	51.78	48.12
9	1	1	-1	-26.22	-19.95
10	-1	-1	1	50.3	52.50
11	0	-1	1	38.92	44.57
12	1	-1	1	-11.87	-11.26
13	-1	0	1	65.08	64.13
14	0	0	1	51.48	50.22
15	1	0	1	-13.81	-11.57
16	-1	1	1	72.95	75.75
17	0	1	1	59.44	55.88
18	1	1	1	-13.09	-11.88

Table 3 Significance of regression coefficient for antioxidant character (%DPPH inhibition)

Coefficients	t Stat	p -value	
β_0	46.34	19.53	2.31E-07
β_1	-34.85	-26.81	2.58E-08
β_2	5.66	4.35	3.34E-03
β_3	3.88	3.66	8.09E-03
β_{12}	-9.12	-5.73	7.15E-04
β_{13}	-3.00	-2.31	5.44E-02
β_{23}	1.33	1.03	3.39E-01
β_{11}	-23.95	-10.64	1.42E-05
β_{22}	-1.49	-0.66	5.30E-01
β_{33}	0.000	-	-
β_{123}	3.15	1.98	-

The coefficients β_{23} , β_{22} and β_{33} are small so the corresponding terms can be neglected. The equation becomes:

$$Y_i = 46.34 - 34.85x_1 + 5.66x_2 + 3.88x_3 - 9.12x_1x_2 - 3.00x_1x_3 - 23.95x_1^2 + 3.15x_1x_2x_3 \quad (3)$$

The verification of this relation was done by comparing the experimental values with the predicted value. The agreement of these values is illustrated by the high value of the correlation coefficient squared (0.9940). It also indicates that most of the variation of the response data is explained by the different input values.

Analysis of response surfaces

The relationship between independent and dependent variables is illustrated in three-dimensional representation of the response surfaces generated by the models for the antioxidant character. As well as multiple regression coefficients, the graphs show a weaker influence of extraction time and hydrolysis temperature between 2-4 h and respectively 60-80°C. The largest slope of the surface is due to the percentage of ethanol in the extraction solvent (Figs. 1 and 2). This is the most influential factor of the process in the studied intervals.

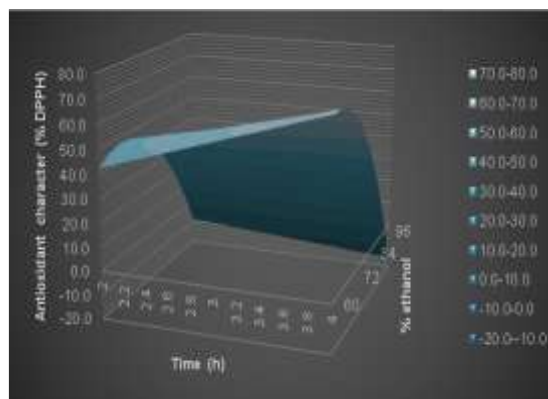


Fig. 1 Response surface plot showing the effect of extraction time and ethanol concentration at a constant hydrolysis temperature course of 70°C, on antioxidant character of extract from flax seeds.

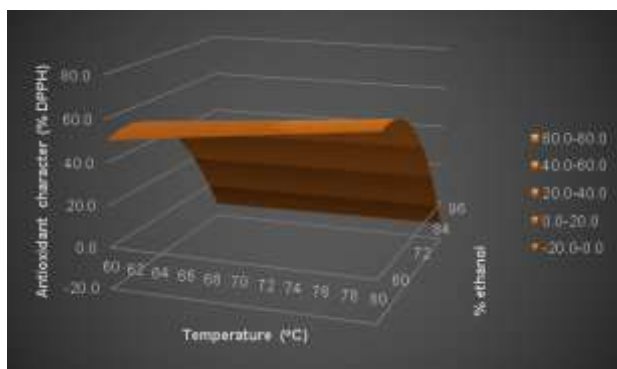


Fig.2 Response surface plot showing the effect of hydrolysis temperature and ethanol concentration at a constant extraction time course of 3 h, on antioxidant character of extract from flax seeds.

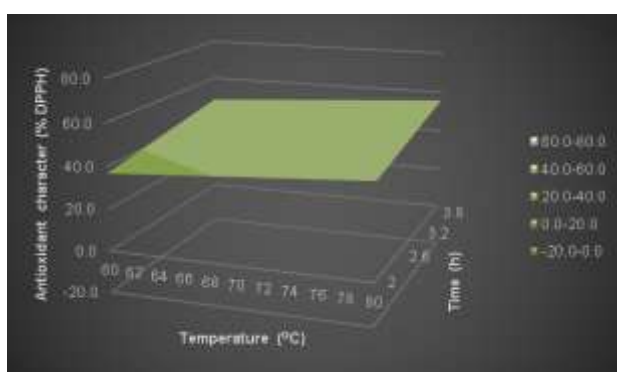


Fig.3 Response surface plot showing the effect of hydrolysis temperature and extraction time at a constant solvent composition course of 80% ethanol, on antioxidant character of extract from flax seeds.

The coordinates of the highest points on the surfaces correspond to the values of the factors that ensure the maximum antioxidant character of extract. The surface in the Fig.3 indicates that the maximum is reached at a marginal point: extraction time (X_2 , 4 h) and hydrolysis temperature (X_3 , 80°C). The curvature of the response surface on the axis of the extraction solvent shows that the maximum is obtained within the range, at a composition over 60% ethanol (X_1). This maximum point can be calculated by equalling with zero the partial

derivative in relation to x_1 of the function (2) for $x_2=1$ and $x_3=1$. Equation (3) becomes:

$$Yi_{(x1)} = 55.88-43.82 x_1-23.95x_1^2 \quad (4)$$

$$Y'i_{(x1)} = -43.82-47.90x_1 = 0 \quad (5)$$

$$x_1 = -0.9149$$

$$X_1 = 61.7 \% \text{ ethanol}$$

$$Yi_{max} = 75.9 \pm 4.5 \% \text{ DPPH inhibition}$$

Using this calculation technique can determine the coordinates for any maximum point placed on the surface ridge (Figs. 1 and 2). For example, the maximum level of antioxidant character and the optimal alcohol concentration can be calculated for the situation in which, to save energy and time, is working on $X_2=2h$ and $X_3=60^\circ C$. In this case, the encoding is $x_2=-1$ and $x_3=-1$. Equation (3) becomes:

$$Yi_{(x1)} = 36.80-19.58 x_1-23.95x_1^2 \quad (6)$$

$$Y'i_{(x1)} = -19.58-47.90x_1 = 0 \quad (7)$$

$$x_1 = -0.4088$$

$$X_1 = 71.8 \% \text{ ethanol}$$

$$Yi_{max} = 40.8 \pm 4.5 \% \text{ DPPH inhibition}$$

Such a reduction in energy consumption substantially reduces the antioxidant character of the extract (from 75.9 to 40.8 % DPPH) and requires solvent with a higher concentration of ethanol (71.8 % instead of 61.7%). It is a convenient situation because more concentrated alcohol is recirculated with less energy and time. For optimal management of the process in any intermediate variant of the above extremes, nomograms can be used (Figs. 4 and 5). These can be calculated and plotted for the entire code palette using the regression function (2) and its partial derivatives. MS Excel 2019 software is enough to achieve this. E.g., for a moderate reduction of energy consumption ($X_2=3.1$ h and $X_3=73.9^\circ C$), the graphical method indicates an optimal value $X_1=64.6$ % ethanol (Fig.4) which determines an antioxidant character of the

extract $Y_{i_{max}} = 62.8 \pm 4.5$ % DPPH inhibition (Fig.5).

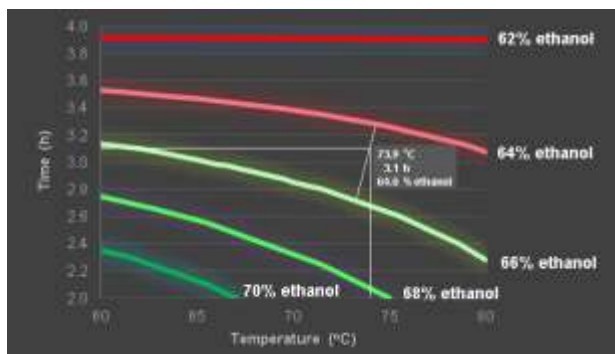


Fig.4 The nomogram with level curves of the optimal ethanol concentration (which ensures a maximum antioxidant character for the extract) according to temperature and time.

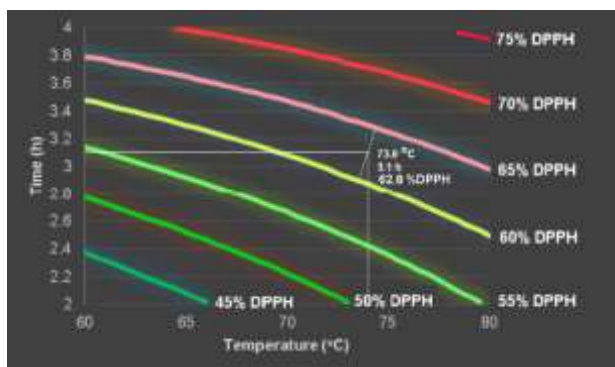


Fig.5 The nomogram with level curves of the antioxidant character according to temperature and time, using an optimal ethanol concentration.

It could thus be established how much temperature and time can be reduced without the antioxidant character being substantially affected.

CONCLUSIONS

The multiple regressions and the response surface methodology were successfully employed to control the antioxidant character of alcoholic extract from flax seeds. The influence of the three factors on the studied intervals decreases in order: solvent ratio ethanol > extraction time > hydrolysis temperature. The experimental design and data processing described herein may constitute a management model of an optimal industrial extraction processes from flax seeds.

ACKNOWLEDGEMENTS

Part of this work was supported by a grant of the Romanian Ministry of Education and Research, CNCS - UEFISCDI, project number PN-III-P1-1.1-PD-2019-0349, within PNCDI III.

REFERENCES

- Chen, J., Liu, X., Shi, Y.P. and Ma, C.Y., 2007. Determination of the Lignan Secoisolariciresinol Diglucoside from Flaxseed (*Linum Usitatissimum L.*) by HPLC. *J. Liq Chrom. & Rel. Technol.*, 30(4): 533-544.
- Home Page of Excel 2019 can be found under <https://support.office.com/en-us/excel>
- Home Page of NIST/SEMATECH 2013 e-Handbook of Statistical Methods can be found under <http://www.itl.nist.gov/div898/handbook/>
- Kedare, S.B. and Singh, R.P., 2011. Genesis and development of DPPH method of antioxidant assay. *Journal of Food Science and Technology*, 48(4): 412-422.
- Lupitu, A. and Dinca, N., 2019. An experimental design for phenolic compounds extraction from flax seeds. *Scientific and Technical Bulletin, Series: Chemistry, Food Science and Engineering*, 16: 8-12.
- Metzner Ungureanu, C.-R. et al., 2020. Investigation on high-value bioactive compounds and antioxidant properties of blackberries and their fractions obtained by home-scale juice processing. *Sustainability*, 12(14): 5681.
- Myers, R. H., & Montgomery, D. C., 2002. Response surface methodology: Process and product optimization using designed experiments (2nd ed.). New York: Wiley.
- Nishizawa, M., Kohno, M., Nishimura, M., Kitagawa, A. and Niwano, Y., 2005. Non-reductive scavenging of 1, 1-diphenyl-2-picrylhydrazyl (DPPH) by peroxyradical: a useful method for quantitative analysis of peroxyradical. *Chemical and Pharmaceutical bulletin*, 53(6): 714-716.
- Parry, J. et al., 2005. Fatty acid composition and antioxidant properties of cold-pressed marionberry, boysenberry, red raspberry, and blueberry seed oils. *Journal of agricultural and food chemistry*, 53(3): 566-573.
- Popova, I.E., Hall, C. and Kubatova, A., 2009. Determination of lignans in flaxseed using liquid chromatography with time-of-flight mass spectrometry. *J Chromatogr A.*, 1216(2): 217-229.

- Sánchez-Moreno, C., 2002. Methods used to evaluate the free radical scavenging activity in foods and biological systems. *Food science and technology international*, 8(3): 121-137.
- Shahidi, F. and Ambigaipalan, P., 2015. Phenolics and polyphenolics in foods, beverages and spices: Antioxidant activity and health effects – A review. *Journal of Functional Foods*, 18: 820-897.
- Willfor, S.M., Smeds, A.I. and Holmbom, B.R., 2006. Chromatographic analysis of lignans. *J Chromatogr A*, 1112: 64-77.



Open Access

This article is licensed under a Creative Commons Attribution 4.0 International License, which permits use, sharing, adaptation, distribution and reproduction in any medium or format, as long as you give appropriate credit to the original author(s) and the source, provide a link to the Creative Commons license, and indicate if changes were made. The images or other third party material in this article are included in the article's Creative Commons license, unless indicated otherwise in a credit line to the material. If material is not included in the article's Creative Commons license and your intended use is not permitted by statutory regulation or exceeds the permitted use, you will need to obtain permission directly from the copyright holder.

To view a copy of this license, visit <http://creativecommons.org/licenses/by/4.0/>.

STUDENTS KNOWLEDGE ASSESSMENT CRITERIA

Simona GAVRILAŞ

Faculty of Food Engineering, Tourism and Environmental Protection, "Aurel Vlaicu" University of Arad, Romania, 2 Elena Drăgoi, Arad 310330, Romania
Corresponding author email: simona2213@yahoo.com

Abstract: Grading reflects the students training level. Its rate, the correlation between the objectives of the course and the student's preparation can be determined by an efficient assessment system. Based on these information, different approaches of the educational model can be followed. The evaluation has three important functions: **classification** and **selection**, ranking students, by providing them indirect recommendations to society, in order to choose and occupy positions in production; **educational**, aspect considered by many researchers, and which influences the mental and intellectual development of learners, forms the principles and skills, acts on the affective-emotional-motivational side; **social**, regarding the influence of society on the results. Students thus know the school requirements. Learn to self-appreciate, to self-evaluate. Evaluation by grading becomes an instrument of their conduct for a certain period. The correct appreciation is stimulating. Evaluation exerts educational influence on students' aspirations and interests and at the same time on the teacher, by regulating and self-regulating the pedagogical behaviour. The evaluation brings the element of novelty, being related to certain criteria. It must be done in relation to the pedagogical objectives of learning, forming a continuous cycle: from it one starts, to it one returns. In modern pedagogy this idea become a fundament. In relation to what is pursued, the learning contents, the means, the forms of development of the educational activities and those of evaluation are established.

Keywords: performance, education, success, objectives

INTRODUCTION

The evaluation problem appeared as a necessity with the advent of the education system. Its importance led to the research orientation of pedagogues, psychologists, sociologists, and resulted in the emergence of a new pedagogical branch, *docimology*, the science of evaluating¹. The term came from Greek, *dokime*, meaning *test*, and *logos* science. Over time this term has been extended, defining the science that investigates examination and grading in various evaluation tests, with the aim of improving them². Didactic evaluation is presented as a feedback process. The educator transmits information to the student, he must decode it and depending on his way of understanding it, retransmit a response to the initiator. Depending on the answer received, he can adjust the way of communicate the initial information or send another one. The feedback process permanently regulates the interaction between the student and the teacher, in order to adopt the appropriate informational shape to the learner understanding level.

Evaluation includes measurement and appreciation but has a more comprehensive idea than these. It refers to the whole concept of

quantification and estimation of the results, completing it by establishing the successful and critical elements, as a basis for improving the verified activity.

In relation to the educational objectives, the evaluation must allow the educator to determine *the moment in which the student can move to another academic objective* but also the *moment of school failure*. Fixing the educational objectives at which most students do not obtain school performance will contribute to the self-control of the teaching processes. It will contribute to improve the teaching methods used, to the way of organizing and carrying out the specific activities.

To estimate what have been achieved during the lesson is necessary to use proper measurement instruments. The suitable techniques to determine the performance achieved are established in the same time with the lesson objective and the content. They will provide qualitative and quantitative objective data about the results obtained. This approach offers the possibility to appreciate what has been appropriated learnt during the studding activity, the registered yield, as well as the adoption of measures to improve the educational process. To

claim that an evaluation of the teaching results can be undertaken without well-developed measuring elements is a serious mistake.

The measuring instruments can take a variety of forms such as: *oral tests*, *written tests*: questions that are expected either answers built by students or choice answers based on those suggested by the teacher, essays, exercises and problems, completions of lacunar texts, schemes, or tables, translations in drawings or schemes of some knowledge; *tests of knowledge* (non-standardized) composed by the teacher, *diagnostic tests*-highlighting gaps and mistakes; *aptitude test*, *performing technical operations* and *measurements*, *making objects* and *other types of tests*.

Regardless of which measurement procedures will be used, it will be developed in terms of criteria that will allow the comparison of the results obtained with the proposed objectives. Based on these analogies the teacher will be able to determine if the results are or not satisfying, if they meet the expectations in terms of school performance. Proceeding in this way the educator can decide whether or not the objectives of the lecture are achieved, if the lesson has succeeded in its entirety.

To appreciate means to be able to establish *till* what level the obtained results correspond to the criteria taken into account. This will return the student's degree of understanding the topic. The feedback through the medium of evaluation may also generate other teaching approaches of the considered subject, by using another auxiliary learning aids.

In the views of modern didactics, the evaluation is made by reference to the objectives of the lecture considered at the same time "*success criteria*". The clearer and more precisely they will be defined, the more objective and conclusive the evaluation will be. So, when we set the objectives, we also have the assessment criteria. A specific characteristic of the performance evaluation must be the development of some appropriate standards³. Establishing the reference points for the educational activity gives an objective overview of all the process. Such an approach will help determine the extent to which the objectives planned reach the proposed target and what changes need to be made in order to increase the

positive aspects appointed and to limit until total elimination the observed deficiencies⁴.

In terms of quality, success or failure is expressed by absolute appreciations: all or nothing, the presence or absence of quality. For example: *the definition of a specific term is known or not*; *the formula of a chemical compound is written correctly or not*; *the operation mode with a measuring instrument is known or not*.

In terms of quantity, the requirements vary in relation to the teaching situation, the progress of students and the complexity of tasks. Of course, not everything can be evaluated immediately, not all results are easy to notice and measure. For example, *the objectives regarding the formation of positive skills towards learning and work*, *collective spirit*, *intellectual curiosity* and *others* cannot be operationalized, specifying by what concrete behaviours of the students could be manifested in this sense. By observation, however, it can be monitored to some extent, whether or not some students show behaviours symptomatic of the attitude in question. The involvement in the learning specific activities will be much greater in the conditions in which the trust in the teacher is developed and strengthened⁵. Similar behaviour has been observed also in case of teamwork, the members ability to rely on each other knowledge and competence abilities contributes to develop novel work directions⁶.

School assessment is imposed as a necessity of the fact that it fulfils certain *functions*⁷:

- *control*, in order to ascertain the level of effectiveness of the teacher's activity;
- *classification* and *selection*, necessary to provide the companies with the right specialists for the different sectors of activity;
- *social*, through school evaluation ensuring the preparation of the student for fast and efficient integration in work and in life;
- *educational*, individual assessment contributes to self-knowledge;
- *didactic*, the evaluation can intervene in the regulation of one's own activity, by choosing at every moment the appropriate methods and procedures, adapting the forms of

organizing the educational process to the particularities of each group of students.

At the level of the lesson, the immediate results and performances are measured, it is true, but nevertheless cannot escape attention the more subtle, more imperceptible effects that accumulate in time, such as *changes of attitude, formation of beliefs, development of certain interests, opinion modelling, opinions* and others. Although we do not have adequate measuring instruments for these effects, the teacher's careful and tireless observation of students' behaviours and communication with them can favour some information and impressions useful for an evaluation, of course much more subjective than in the case of appreciation of knowledge or practical skills.

Different studies suggested the positive effect of the collegial student's assessment, underlining the importance of the informal support^{8, 9}. This approach contributes to improvement of student involvement in the learn process⁹.

The various measurement tests can be applied at the beginning, throughout or at the end of the lesson.

The paper aim is to emphasize some general aspect of the student assessment procedure. There are underlined some critical directions that should be considered during the evaluation criteria establishment: *which are the important points that may contribute to a successful learning activity from its perspective?* There are summarised a few examples of good practice models which have proved to be efficient and some factors that contributes learning improvement.

METHODS

When the evaluation is made based on the comparison with the initial situation from which we started we are dealing with the *comparative evaluation*.

When the evaluation identifies only the changes that occurred within some directly targeted behaviours, we are dealing with the *absolute evaluation*.

As for the act of evaluation taken in all its aspects, as a *measurement* and *appreciation* at the same time, it has always been an essential aspect but also a difficult problem to solve^{10, 11}.

Traditional education considered necessary to separate the moment of verification and evaluation from that of learning and teaching¹². Currently, the changes in optics that have taken place in this matter tend to integrate assessment into the teaching and learning process itself, where it is more appropriate and natural to be placed and not considered as something outside the training process in which they are engaged constantly the teacher and the student. A challenging method could be represented by integration of the assessments bases into the student's system of knowledge. This approach won't be easy to apply in the traditional educational system, due to the fact that is based on collaboration and cooperation between all the parts implicated, student-teacher. From modern teaching perspective, the provocation can be determined especially by the high number of students, situation which limit the direct interaction time and the feedback¹³.

Attempts have been made lately to suppress the classic moment of verification at the beginning of the lesson, questions, questionnaires, other ways of verification. These will be normally integrated in the method itself after which the new lesson is taught, that is, the conduct of the lesson should inherently include continuous assessment^{14, 15}. In this way more corrective techniques could be applied, to support students who encounter different learning difficulties. Everything must be done for the examination of previously acquired information's to be carried out during the active exploration of new knowledge. In this way it is possible to avoid the unproductive use of teaching time at the beginning of the activity, when only a few students are involved, the others being "tormented" by inactivity.

RESULTS AND DISCUSSIONS

For evaluation to be effective, it must be based on certain principles:

- *continuous* and *consistent*, in order to be able to see through it, the evolution, the rhythm achieved by each student;
- to be *in accordance* with the general instructive-educational objective but also of each discipline;
- be *carried out* in the form of a system of evaluation techniques;

- to be *objective* and *main* to provide a real total of the student's level of preparation at a given time;
- to be based on a system of *unitary* and *consistent requirements*;
- *maintaining* the same evaluation criteria.

There are different possibilities for evaluation¹⁶:

- *evaluation by reference to the norm* that provides us with information about the relative ranking of individuals, a hierarchy within the group ("upper"-above the class average, "middle", "below average"-weak);
- *evaluation by reference to the subject*, to the content of the programs;
- *evaluation by reference to criteria*, such as objectives.

The most common form of evaluation is grading. It can be group or individual. It must consider the possibilities of each individual student. This way of grading is used in the conditions in which the instructive-educational act is not carried out on classes but on groups of students, organized on the basis of the passive criterion of capacities.

Studies performed in domain of formative appreciation open the idea of a constructive path which might be followed. The approach is not easy to follow, it involves the active involvement of both students and teachers, in a constructive and reasoned dialogue¹⁷.

Importance for objective evaluation in higher education presents the development of formal criteria. The inclusion of assay criteria can contribute to the improvement of the obtained results¹⁸.

By evaluation the results are quantified receiving numerical values that possess the properties of real numbers of arithmetic and are expressed in notes from 10 to 1.

The school grade includes a large dose of subjectivity, its sources being related to the teacher, the field of education and the student. The analysis of these sources in relation to the school grade, as an evaluation tool, leads to the following findings that could also influence it¹⁹:

- the well-known *Oedipal effect* can sometimes be observed. This effect consists in the fact that some educators grade the student on

the basis of a conviction he has formed in connection with it.

- *individual error*, when the educator applies the same assessment criteria, but differently in relation to each learnable, or applies different criteria in relation to each student or discipline.

In students grading can be often observed the contrast effect. Subjectivity is generated by logical error. Some educators are willing to appreciate less the content, the quality of an answer and more the order, accuracy, effort made by the student. Subjectivity is also determined by the fact that for some objectives the grading can be done exactly, in others not, and also by the student's ability to formulate answers at a given time. It depends not only on the mode of assimilation but also on factors such as the state of the moment, the level of fatigue, the conditions of certain mental processes.

In general, the grading criterion is also based on the requirements of the curriculum, even if in some cases it may be considered insufficient or incomplete.

As signs of appreciation, the grades do not remain without echo in the students' consciousness, becoming educative from many points of view. For example, getting used to being rigorously graded, students begin gradually, gradually, to realize the university requirements, to become aware of the criteria according to which they are appreciated, to internalize the teacher's recognition. Over time, they will begin to relate to these criteria on their own, to appreciate themselves. The evaluation coming from outside will thus gradually turn into self-evaluation. The student's capacity of precise self-evaluation can help them to adopt the appropriate learning method²⁰. The more objective and correct the assessment is, and less influenced by different arbitrary subjective factors, the more stimulating it will become and the more it will be able to energize the learning efforts.

With the communication of the assessment result, the student must be helped to become aware of the positive or negative aspects that justify it.

The evaluation tools include a diversity of forms, the examples appeared in the specialized

literature remaining indicative, the practice and the living experience of the teacher must always complete and update the forms of appreciation and measurement.

The tools used depends on the skill and training of the teacher in this regard, the group of students to which it applies and the topic or subject to which the knowledge assessment is made.

Another assessment approach, with significant good results regarding also the level of informational acquisitions is where students elaborated the own evaluation criteria²¹.

For an efficient evaluation the grading criterion must be correlated with other assessment criteria. Starting from the idea that work represents the decisive factor that created man, it means that it can and must be one of the criteria of appreciation, in its essence the fundamental form of learning.

The purpose of the instructive-educational process is to prepare the individual for himself and the society. An objective evaluation correlates the student effort regarding quality and quantity of personal involvement in the educational process. The same task can be accomplished at the same school level, but through different effort. Neglecting such aspect can have negative impact on student subsequent implication degree in learning activities.

CONCLUSIONS

The elaboration of some worksheets involves a certain methodology that obliges the teacher to ensure some essential qualities for any tests:

- to be adequate to the objectives and subjects studied;
- to be effective and for this valid;
- to be accurate, meaning to really reflect the knowledge degree;
- be practical, meaning easily applicable;
- the expected score to depend on how well the student knows, not how fast he responds.

REFERENCES

- ¹Bantaş, A., 2008. Dicționar englez-român, roman-englez. Editura Teora, pp. 621.
- ²Oliveira, A., Lenartovicz, L., 2018. School Evaluation: A Possible Dialogue between the History and Epistemology. Open Journal of

Social Sciences 6, 179-189. doi: 10.4236/jss.2018.68014.

³Trevisan, M.S., Davis, D.C., Calkins, D.E., Gentili, K.L., 2013. Designing Sound Scoring Criteria for Assessing Student Performance. The Research Journal For Engineering Education, <https://doi.org/10.1002/j.2168-9830.1999.tb00415.x>.

⁴Harlen, W., 2007, Criteria for evaluating systems for student assessment. Studies in Educational Evaluation 33, 15-28.

⁵Leighton, J. P., Seitz, P., Chu, M-W., & Bustos Gomez, M. C., 2016. Operationalizing the role of trust for student wellbeing, learning and achievement. International Journal of Wellbeing 6(2), 57-79. doi:10.5502/ijw.v6i2.467.

⁶Ness, I.J., Hanne Riese, H., 2015, Openness, curiosity and respect: Underlying conditions for developing innovative knowledge and ideas between disciplines. Learning, Culture and Social Interaction 6, 29-39.

⁷Kari Smith, K., 2016. Functions of Assessment in Teacher Education. In book: International Handbook of Teacher Education, pp.405-428, DOI: 10.1007/978-981-10-0369-1_12.

⁸van Hattum-Janssen, N., Lourenço, J.,M., 2011. Explicitness of criteria in peer assessment processes for first-year engineering students. European Journal of Engineering Education 31 (6), 683-691, <https://doi.org/10.1080/03043790600911779>.

⁹Bloxham, S., West, A., 2007. Learning to write in higher education: students' perceptions of an intervention in developing understanding of assessment criteria. Teaching in Higher Education, Critical Perspectives 12 (1), 77-89, <https://doi.org/10.1080/13562510601102180>.

¹⁰Yaron Ghilay, Y., Ghilay, R., 2012. Student Evaluation in Higher Education: a Comparison Between Computer Assisted Assessment and Traditional Evaluation. British Journal of Educational Technology 9(2), 8-16, DOI: 10.26634/jet.9.2.1942

¹¹Khorsandi, M. Kobra, A., Ghobadzadeh, Mc., Kalantari, M., Seifei, M., 2012. Online vs. traditional teaching evaluation: a cross-sectional study. Procedia-Social and Behavioral Sciences 46, 481-483, doi: 10.1016/j.sbspro.2012.05.145.

¹²Quansah, F., 2018. Traditional or Performance Assessment: What is the Right Way in Assessing Learners?. Research on Humanities and Social Sciences 8(1), 21-24.

¹³Rust, C., Price, M., O'donovan, B., 2003. Improving Students' Learning by Developing their Understanding of Assessment Criteria and Processes. *Assessment & Evaluation in Higher Education* 28 (2), DOI: 10.1080/0260293032000045509.

¹⁴Seifu, W.G., 2016. Assessment of the implementation of continuous assessment: the case of METTU university. *European Journal of Science and Mathematics Education* 4(4), 534-544.

¹⁵Xiong, Y., Hoi K. Suen, H.K., 2018. Assessment approaches in massive open online courses: Possibilities, challenges and future directions. *International Review of Education* 64, 241-263.

¹⁶Prieto Barrio, M.I., Cobo Escamilla A., González García M.N, Moreno Fernández, E., Pilar de la Rosa García, P., 2015. Influence of assessment in the teaching-learning process in the higher education. *Procedia-Social and Behavioral Sciences* 176, 458-465.

¹⁷Hansen, G., 2020. Formative assessment as a collaborative act. Teachers' intention and students' experience: Two sides of the same coin, or? *Studies in Educational Evaluation* 66, 100904.

¹⁸Meyer-Beining, J., 2020. "Of course we have criteria" Assessment criteria as material semiotic means in face-to-face assessment interaction. *Learning, Culture and Social Interaction* 24, 100368.

¹⁹Izci, K., 2016. Internal and External Factors Affecting Teachers Adoption of Formative

Assessment to Support Learning. *International Journal of Social, Behavioral, Educational, Economic, Business and Industrial Engineering* 10(8), 2541-2548, waset.org/Publication/10005201.

²⁰Hoseina, A., Harle, J., 2018. The relationship between students' prior mathematical attainment, knowledge and confidence on their self-assessment accuracy. *Studies in Educational Evaluation* 56, 32-41.

²¹Chiu-Lin, L., Gwo-Jen, H., 2015. An interactive peer-assessment criteria development approach to improving students' art design performance using handheld devices. *Computers & Education*, 85, 149-159.



Open Access

This article is licensed under a Creative Commons Attribution 4.0 International License, which permits use, sharing, adaptation, distribution and reproduction in any medium or format, as long as you give appropriate credit to the original author(s) and the source, provide a link to the Creative Commons license, and indicate if changes were made. The images or other third party material in this article are included in the article's Creative Commons license, unless indicated otherwise in a credit line to the material. If material is not included in the article's Creative Commons license and your intended use is not permitted by statutory regulation or exceeds the permitted use, you will need to obtain permission directly from the copyright holder.

To view a copy of this license, visit <http://creativecommons.org/licenses/by/4.0/>.

HIGH RESOLUTION MASS SPECTROMETRY WITH CHIP-BASED IONIZATION FOR THE ASSESSMENT OF NONCOVALENT INTERACTIONS OF PROTEINS WITH NORMAL BRAIN AND BRAIN TUMOR GANGLIOSIDES

Raluca ICĂ^{1,2}, Mirela SÂRBU¹ and Alina D. ZAMFIR^{1,3}

¹National Institute for R&D in Electrochemistry and Condensed Matter, Timisoara, Romania

²Faculty of Physics, West University of Timisoara

³“Aurel Vlaicu” University of Arad, Romania

Corresponding author email: alina.zamfir@uav.ro

Abstract: The noncovalent interactions between the amyloid beta ($A\beta$) and α -synuclein (Syn) proteins with native gangliosides extracted and purified from human brain and human glioma were studied using an analytical platform encompassing fully automated chip-nanoelectrospray (nanoESI) on a NanoMate robot coupled to a quadrupole time-of-flight (QTOF) mass spectrometer (MS). The novel interaction assays developed here for this purpose involved several stages: i) the incubation at 37°C under constant steering of the protein and gangliosides in 10 mM ammonium acetate buffer, pH 6.0, up to a concentration of 1 pmol μL^{-1} and 10 pmol μL^{-1} , respectively; ii) collection of aliquots directly into the 96-well plate of the robot after 1, 5, 10, 15, 30, 60 and 180 min of incubation and iii) immediate submission of the reaction products to MS screening and structural analysis. Chip-nanoESI QTOF MS and CID MS/MS revealed the formation of the $A\beta$ -GT1(d18:1/18:0) and $A\beta$ -GT1(t18:1/18:0) complexes as well as the preferential binding of Syn to GD1, GT1, GQ1 and GO1 species. CID MS/MS top-down fragmentation analysis demonstrated that the $A\beta$ protein binds to a GT1b isomer type structure, characterized by Neu5Ac linkage to the external galactose and a disialo element Neu5Ac-Neu5Ac bound to the inner galactose of the molecule. Thus, by chip-MS and tandem MS experiments it was possible to deduce the structure of this non-covalent complex as: $A\beta$ -GT1b (d18:1/18:0). Similar results were obtained also for the $A\beta$ complex formed with the gangliosides having trihydroxylated ceramide as well as the complexes of Syn with G1 class of gangliosides.

Keywords: Gangliosides, Noncovalent interactions/complexes, Chip-nanoelectrospray mass spectrometry.

INTRODUCTION

Gangliosides (GGs) represent a particular class of glycosphingolipids with a complex structure consisting of a ceramide (Cer) moiety, of variable composition with respect to the types of sphingoid base and fatty acid residues, glycosidically linked to an oligosaccharide chain containing one or more sialic acid units. Gangliosides are present in all mammals, both in tissues and body fluids, systematic quantitative analyses have demonstrated that the highest concentration is found in the central nervous system: brain, spinal cord and cerebrospinal fluid. In brain tissue, for instance, gangliosides represent 6% of the total mass of lipids [1]. GGs mediate vital biological processes through non-covalent

intermolecular interactions. To understand the structure, function relationship at the molecular level for each GG structural entity involved in a physiological/pathological process and to improve the therapeutic significance, it is necessary to determine their interactions in detail using the most accurate methods of analysis. Mass spectrometry (MS) has lately become a method of choice due to its capability to detect minor species in complex mixtures with an unsurpassed sensitivity [2,3].

The development of MS techniques which, due to superior sensitivity, selectivity, resolution, reproducibility and analysis speed represent nowadays the state-of-the-art in bioanalytics, has led to important findings in glycolipidomics, a vast number of glycolipid

isomers, isobars, and conformers were not only discovered *de novo*, but could also be associated to severe disorders and malignant transformations [4,5] and studied as high-affinity ligands for certain proteins [3,6]. In this context, we report here upon the development of a strategy for studying the noncovalent protein-ganglioside interactions. The interaction was monitored using fully automated chip-nanoelectrospray ionization (nanoESI) on a NanoMate robot in laboratory coupled to a quadrupole time-of-flight (QTOF) mass spectrometer.

MATERIALS AND METHODS

I) INTERACTION PRECURSORS

A) Amyloid beta protein sequence from Merck KGaA (Darmstadt, Germany): (A β 1-40) Amyloid β Protein Fragment, (molecular weight, MW: 4329.82 Da) derived from the amyloid- β protein (A β), *DAEFR HDSGY EVHHQ KLVFF AEDVG SNKGA IIGLM VGGVV* in interaction with a native GG mixture extracted from normal adult (45 y.o.) human brain.

B) Human recombinant α -synuclein (Syn 1-140, MW: 14459.70 Da) from Merck KGaA (Darmstadt, Germany) having the following amino acid sequence: *MDVFM KGLSK AKEGV VAAAE KTKQG VAEAA GKTKG GVLVVG SKTKE GVVHG VATVA EKTKE QVTNV GGAVV TGVTA VAQK T VEGAG SIAAA TGFVK KDQLG KNEEG APQEG ILEDM PVDPD NEAYE MPSEE GYQDY EPEA* in interaction with a native GG mixture extracted and purified from human glioma.

II) CHIP-BASED MASS SPECTROMETRY

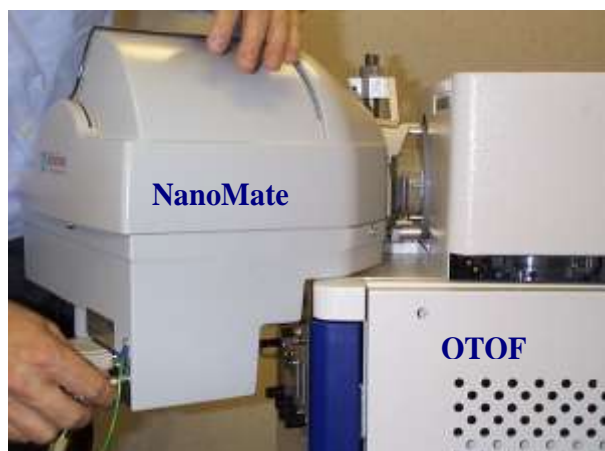


Figure 1. Chip-based nanoelectrospray, NanoMate™ robot incorporating the 400-nozzle ESI Chip technology (Advion BioSciences, Ithaca, USA) in laboratory coupled to a QTOF MS (Waters, Manchester, UK). The electrospray process was initiated at 1.3 kV applied on the pipette tip and 0.40 psi nitrogen back pressure

III) BINDING ASSAY AND CHIP-MS ANALYSIS OF THE REACTION PRODUCTS

In order to achieve the interaction, a series of testing and optimization experiments using different solvent systems for identifying an appropriate buffer system were carried out. Optimal results were obtained using the ammonium acetate/acetic acid buffer system. A schematic of the workflow is presented in Figure 2.

Briefly, the interaction assay involved the incubation at 37 °C under constant stirring of the protein and gangliosides dissolved in 10 mM ammonium acetate buffer, pH 6.0, to a concentration of 1 pmol μL^{-1} and 10 pmol μL^{-1} , respectively. Aliquots of the reaction products were collected after 1, 5, 10, 15, 30, 60 and 180 min in the 96-well plate of the NanoMate robot and immediately submitted to QTOF MS and MS/MS by CID in positive ion mode.

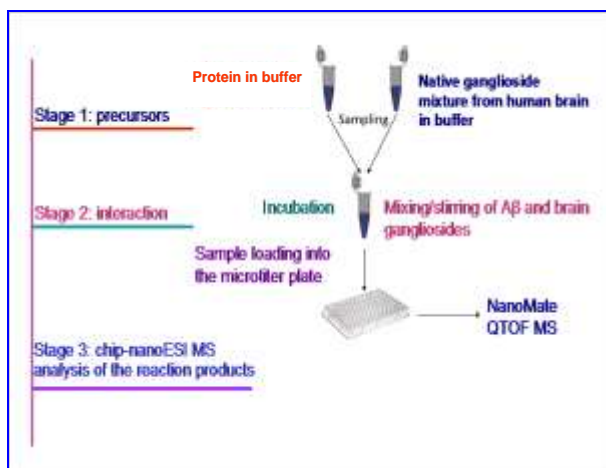


Figure 2. Schematic of the workflow for studying the noncovalent protein-ganglioside interactions by NanoMate-QTOF MS

RESULTS AND DISCUSSIONS

Screening of the A β 1-40 (Figure 3) in buffer revealed two signals, which, according to mass calculation correspond to the triply protonated A β 1-40 (measured MW: 4330.563 Da, mass accuracy: 171 ppm) and to A β 1-41 having the amino acid sequence *DAEFRHDSGYEVHHQKLVFFAEDVGSNKGAIIGLMVGGVV*, which was also detected in the sample as a triply deprotonated molecule at m/z 1482.615 (measured MW: 4445.445 Da).

NanoMate-QTOF MS analysis of the reaction products revealed the formation of four noncovalent complexes of A β (1-40) with GT1(d16:1/18:0), GT1(d18:1/18:0), GT1(t18:1/18:0) and GQ1(d18:1/18:0), all detected as tetraprotonated $[M+4H]^{4+}$ molecules (Figure 4). Interestingly, only complexes with highly sialylated, tri- and tetrasialo GG species were found. These findings do not exclude the possible formation of complexes with GM and GD structures as well, but highlights the possible role of sialylation in protein-ganglioside interactions, which claims for further studies in this direction.

By applying the same protocol for the study of the noncovalent interaction between α -synuclein and GGs extracted from human glioma tumor it could be deduced that α -synuclein formed non-covalent complexes with

the species of G1 class, *i.e.* those species that exhibit the longest glycan chain. Furthermore, a high affinity of α -synuclein protein was observed for polysialylated structures.

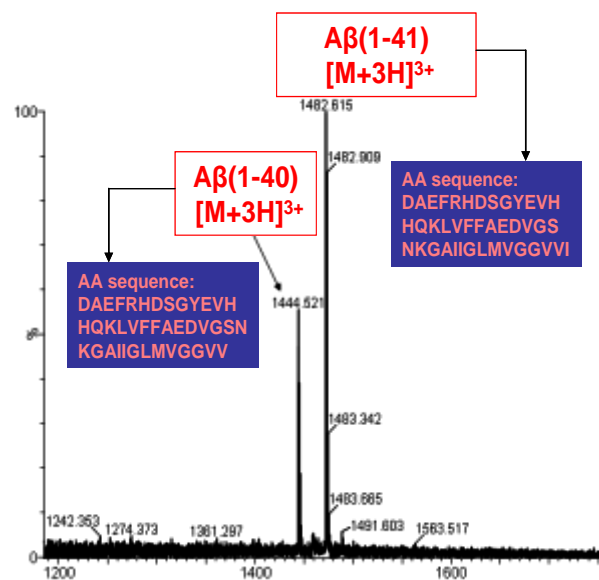


Figure 3. NanoMate-QTOF MS in positive ion mode of the A β protein in buffer. Concentration: 1 pmol μL^{-1} ; acquisition time 2 min. nanoESI: 1.2 kV; cone voltage: 50 V; nitrogen at 0.40 psi. Buffer system: 10 mM ammonium acetate/ acetic acid pH 6.0.

The complexes formed and detected are with GGs containing several Neu5Ac units in the sugar chain, namely GD1, GT1, GQ1 and GO1.

It is noteworthy to mention that some of these species, *i.e.* GO1, a ganglioside species of high sialylation degree that interacted with α -synuclein, could not be detected in glioma by direct nanoESI chip MS screening of the native ganglioside extract, neither in buffer nor in water/methanol, mainly due to the reduced expression of such structures in the tissue; on the other hand, the unusually high complexity of the mixtures, as those extracted from human brain and brain tumors, represents also a factor leading to the difficulty in detection and identification of low abundant species by simple sample profiling by MS.

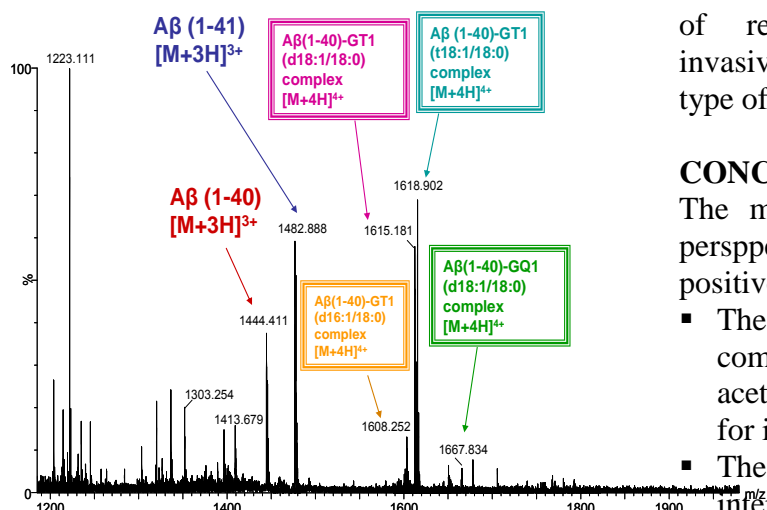


Figure 4. NanoMate-QTOF MS in positive ion mode of the reaction products resulted after 30 min incubation in buffer at 37 °C of A β protein and human brain GG mixture. Acquisition time: 5 min. nanoESI: 1.4 kV; cone voltage: 50 V; nitrogen at 0.40 psi. Buffer system: 10 mM ammonium acetate/acid acetic pH 6.0.

From the biological point of view, these findings reveal that the native GG mixture from glioma contains minor species, previously unidentified and which formed non-covalent complexes with α -synuclein and thus could be identified. Therefore, based on the affinity of proteins for certain species, the method can be used to *de novo* identify components having a low expression in a certain human matrix.

Although α -synuclein protein is most intensively studied in relation to neurodegenerative diseases, recent studies correlate glioblastoma with the overexpression of α -synuclein protein [7]. On the other hand, it was clearly demonstrated a reduction in α -synuclein toxicity in cases treated with GGs and in particular the ability of GM1 monosialo tetraose from G1 class to protect against Syn toxicity *in vivo* [8]. Related to these previous reports, our results indicate for the first time that: a) α -synuclein has affinity for the entire G1 class of gangliosides, not just for GM1 (monosialylated) and b) the entire G1 class should be tested against the toxicity of α -synuclein in gliomas, possibly with the effects

of reducing proliferation/infiltration and invasiveness that characterize the cells of this type of cancers.

CONCLUSIONS

The most important conclusions and future perspectives of the work in the field may be positively summarized as follows:

- The results have demonstrated the compatibility of 10 mM ammonium acetate/acid acetic pH 6.0 as buffer system for interaction and spraying solvent;
- The data collected by noncovalent interaction assays followed by chip-based nanoESI MS suggest for the first time that, exposed to a highly complex mixture of gangliosides under conditions facilitating the interaction, these proteins preferentially bind the G1 ganglioside class, having a particular affinity for polysialylated species GT1 and GQ1;
- Minor species, which might play an important biological role, could be detected via their complex formed with A β or Syn proteins;
- The platform appears as a method of choice not only for the assessment of the noncovalent interactions, but also for the detection and identification of species of low expression in complex mixtures. Certainly, for this purpose, further method refinements are required and planned for the near future.

ACKNOWLEDGEMENTS

This work was supported by the Romanian National Authority for Scientific Research, UEFISCDI through projects PN-III-P1-1.2-PCCDI-2017-0046 and 541PED/2020 granted to ADZ, and postdoctoral PN-III-P1-1.1-PD-2019-0226 project granted to MS.

REFERENCES

- [1] Groux-Degroote, S., Guérardel, Y., Delannoy, P., 2017. Gangliosides: structures,

biosynthesis, analysis, and roles in cancer. *ChemBioChem*. 18, 1146–1154.

[2] Zamfir, A.D., 2017. Microfluidics-mass spectrometry of protein-carbohydrate interactions: applications to the development of therapeutics and biomarker discovery. *Methods Mol. Biol.* 109-128.

[3] Han, L., Xue, X., Roy, R., Kitova, E.N., Zheng, R.B., St-Pierre, Y., Lowary, T.L., Klassen, J.S., 2020. Neoglycolipids as glycosphingolipid surrogates for protein binding studies using nanodiscs and native mass spectrometry. *Anal. Chem.* 92, 14189-14196.

[4] Wang, W.X., Whitehead, S.N., 2020. Imaging mass spectrometry allows for neuroanatomic-specific detection of gangliosides in the healthy and diseased brain. *Analyst* 145, 2473-2481.

[5] Ica, R., Simulescu, A., Sarbu, M., Munteanu, C.V.A., Vukelić, Ž., Zamfir, A.D., 2020. High resolution mass spectrometry provides novel insights into the ganglioside pattern of brain cavernous hemangioma. *Anal. Biochem.* 609:113976. doi: 10.1016/j.ab.2020.113976 (Epub ahead of print).

[6] Bolla, J.R., Agasid, M.T., Mehmood, S., Robinson, C.V., 2019. Membrane protein-lipid

interactions probed using mass spectrometry. *Annu. Rev. Biochem.* 88, 85-111.

[7] Duan, J., Ying, Z., Su, Y., Lin, F., Deng, Y., 2017. α -Synuclein binds to cytoplasmic vesicles in U251 glioblastoma cells. *Neurosci. Lett.* 642, 148-152.

[8] Schneider, J., Aras, R., Williams, C., Koprach, J., Brotchie, J., Singh, V., 2019. GM1 ganglioside modifies α -synuclein toxicity and is neuroprotective in a rat α -synuclein model of Parkinson's disease. *Sci Rep.* 9, 8362-8369.



Open Access

This article is licensed under a Creative Commons Attribution 4.0 International License, which permits use, sharing, adaptation, distribution and reproduction in any medium or format, as long as you give appropriate credit to the original author(s) and the source, provide a link to the Creative Commons license, and indicate if changes were made. The images or other third party material in this article are included in the article's Creative Commons license, unless indicated otherwise in a credit line to the material. If material is not included in the article's Creative Commons license and your intended use is not permitted by statutory regulation or exceeds the permitted use, you will need to obtain permission directly from the copyright holder.

To view a copy of this license, visit

<http://creativecommons.org/licenses/by/4.0/>.

PECTIN QUANTIFICATION FROM CELLULOSIC/LIGNOCELLULOSIC RAW MATERIALS BY FT-IR ATR ANALYSIS

Dorina Rodica CHAMBRE¹, Mihaela DOCHIA^{2*}

¹Faculty of Food Engineering, Tourism and Environmental Protection, "Aurel Vlaicu" University, Romania, 2 Elena Dragoi, Arad 310330, Romania

² Research Development Innovation in Natural and Technical Sciences Institute, "Aurel Vlaicu" University, Romania, 2 Elena Dragoi, Arad 310330, Romania
Corresponding author email: dochiamihaela@yahoo.com

Abstract: This paper presents an accurate quantification by FT-IR ATR analyses of pectin content from cotton and flax raw woven fabrics. For this purpose, the investigated samples were exposed to HCl vapours. The relative absorbance of pectin-specific bands was evaluated. The results showed an increase in the band intensity values located at $\sim 1735\text{ cm}^{-1}$ and a decrease of the one from $\sim 1645\text{ cm}^{-1}$ after the exposure of the samples to HCl vapours due to the transformation of the (COO-) linked with Ca^{2+} groups into acidic carboxylic groups.

Keywords: cotton fabric, flax fabric, pectin, HCl vapours exposure, FT-IR ATR spectroscopy

INTRODUCTION

Due to their renewable character, textile materials based on natural fibres are gaining more and more ground in the framework of sustainable development policy. Their use in various industrial fields (textiles, construction, automobiles, etc.) implies a decrease in fossil fuels that fall within the lines of sustainable development (Karus et al. 2002, Puşcas et al. 2002, Perepelkin et al. 2005).

Cotton and flax materials get into the category of renewable materials, and their investigation, analysis, and characterization to find environmentally friendly processing methods for obtaining value-added materials can be considered a priority.

Cotton occupies one of the first places in the world in production, at the same time having the highest percentage of cellulose in the composition (Eichhorn et al. 2001, Pursley et al. 2005). The lignocellulosic materials like flax have become interesting in the last decade, due to the possibility of cultivation in areas with lower temperatures in Europe as well as the low costs for crop maintenance because no pesticides are needed (Summerscales et al. 2010).

According to literature data, the chemical composition of investigated materials is: cotton - 86-96% cellulose, 0.7-1.9% pectin, 0.4-1.2% waxes, etc. (Wakelyn et al. 2007); flax - 70-75% cellulose, 3-15% pectin, 8-15% waxes and

hemicelluloses, 0.6-4% lignin (Abdel-Halim et al. 2008, Manaia et al. 2019).

Because there are differences in structure, composition, and properties between these raw materials, detailed information on the content of non-cellulosic attendants is needed to find suitable solutions in their processing. For example, pectin, a complex of polysaccharides of 1-4 linked α -D-galacturonic acid molecules, esterified with methanol or as calcium salts (Dochia et al. 2013), must be removed from the substrate to improve the hydrophilic properties of fabrics.

Infrared spectroscopy, due to its versatility, has become one of the most important analytical techniques available to researchers. As shown in previous studies (Dochia et al. 2018a, 2018b, 2018c), the FT-IR ATR spectroscopy can be a simple and rapid technique to obtain data about the structure and constituents of cellulosic and lignocellulosic materials (Dochia et al. 2018a, Wang et al. 2006, Terpáková et al. 2012, Choe et al. 2018, Ouajai et al. 2005). This method allows the identification of specific bands for cellulose and non-cellulosic attendants' functional groups.

Because in the FT-IR ATR spectra there are situations in which the characteristic bands of various vibrations overlap, a specific preparation of the samples (e.g. HCl vapour treatment of natural fibres) is required for a more accurate interpretation of the results (Wang et al. 2006, Choe et al. 2018). At the same time, the FTIR

ATR spectra allow obtaining information related to the amorphous and crystalline structure of the cellulosic polymer from raw materials. This is possible by calculating the Lateral Order Index (LOI) and the Total Crystallinity Index (TCI) using absorbance values (Ciolacu et al. 2011).

The aim of this paper has been the accurate quantification of pectin content from cotton and flax raw woven fabrics by FT-IR ATR analyses. In this purpose, the raw cotton and flax samples were subjected to the action of HCl vapours and the relative absorbance values of pectin specific band were evaluated.

MATERIALS AND METHODS

Materials

Samples from the following fabrics were analysed:

- Raw woven cotton fabric with a width of 150 ± 3 cm, the weight of 200 ± 10 g/m², the warp of 100 % cotton yarn with Ne 25/2 and weft of 100 % cotton yarn with Ne 25/1 (denoted as **RC**);
- Raw woven flax fabric with a width of 120 ± 3 cm, the weight of 220 ± 10 g/m² and 100 ± 1 fibres/10 cm warp and weft density (denoted as **RF**);

Method

The experiments were made on 3 samples taken from different parts of the fabrics. Before being analysed, the samples were conditioned at 105 °C in a Sartorius MA 100 balance. In the case of

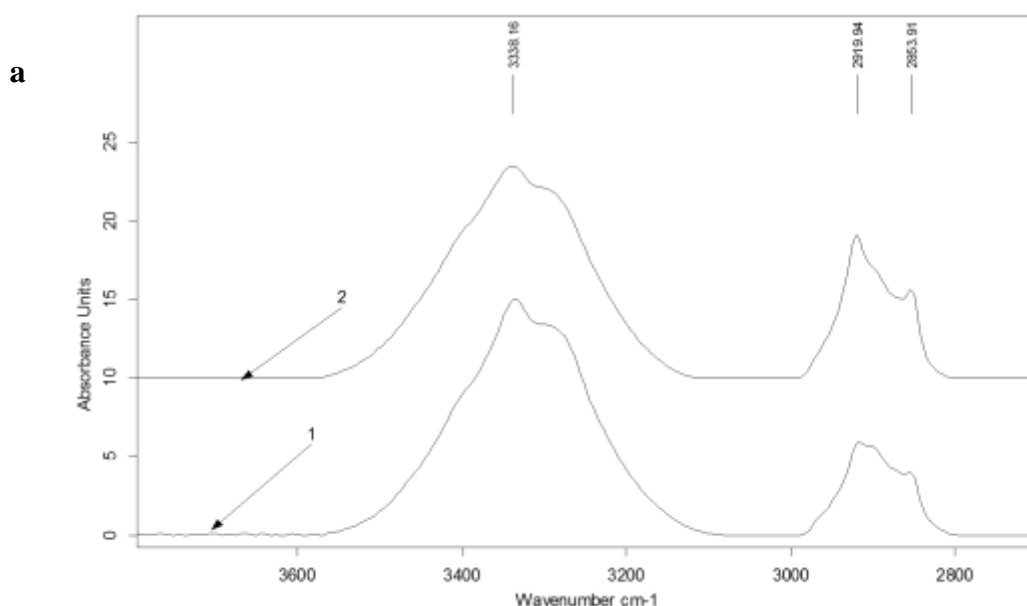
samples subjected to the action of HCl vapours, the time exposure was 1 minute.

FT-IR ATR spectra were obtained with a Bruker Vertex 70 spectrophotometer equipped with the ATR cell. The measurements were carried out on the 600 - 1800 cm⁻¹ and 2600 - 4000 cm⁻¹ wavelength range with a resolution of 8 cm⁻¹ and 100 scans. For the acquisition and processing of data (normalization to the peak at 615 cm⁻¹ and baseline correction), the OPUS software was used. Before each measurement, a background calibration was done.

RESULTS AND DISCUSSIONS

Cotton and flax materials present several specific absorption bands for cellulose and non-cellulosic components (lignin, pectin, etc.). Figure 1 a and b presents the FT-IR ATR spectra of the RC and RF samples recorded on 600 - 1800 cm⁻¹ and 2600 - 4000 cm⁻¹.

The peak at 3338 cm⁻¹ is characteristic of the hydrogen-bonded stretching vibration of the hydroxyl group (OH) from polysaccharides structures (cellulose and hemicellulose). The peaks observed at 2919 cm⁻¹ and 2853 cm⁻¹ are extra bands given by C-H stretching vibration of noncellulosic components like pectin and waxes which overlap with the specific signal of the same vibrations of cellulose and hemicellulose (Terpáková et al. 2012, Choe et al. 2018, Subramanian et al. 2005).



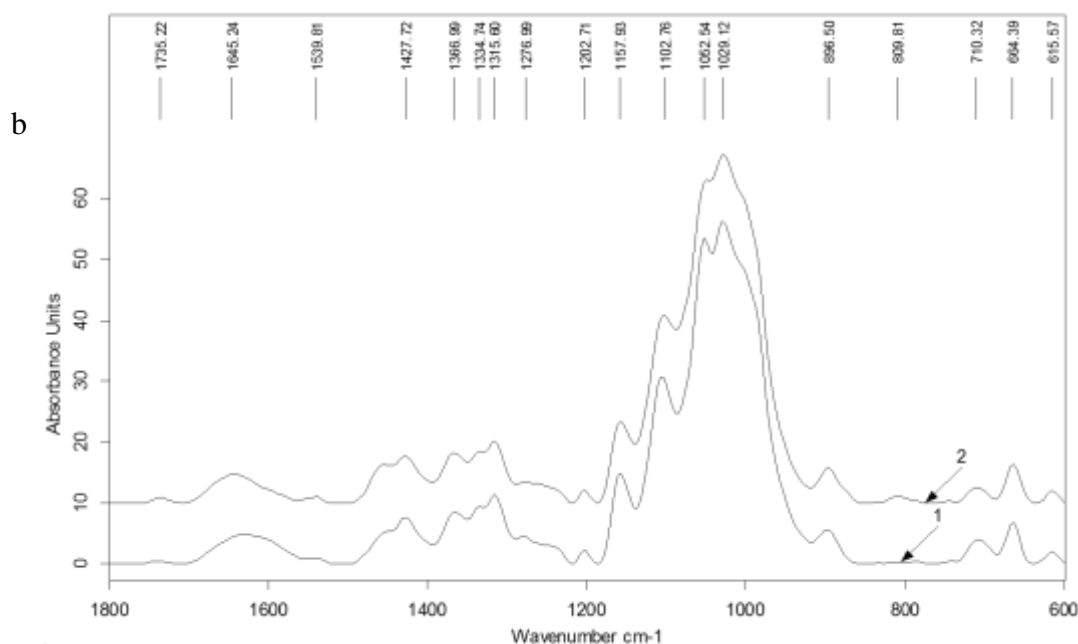


Figure 1. FT-IR ATR spectra of 1- **RC** and 2 - **RF** samples on 2600 - 4000 cm^{-1} range (a) and 600 – 1800 cm^{-1} range (b)

Comparing the extra bands obtained for the two types of samples analysed, it is observed that in the case of flax their intensity is higher than that of cotton. This suggests a higher content of waxes and pectins of the raw lignocellulosic material.

The weak absorbance located in the FT-IR spectrum at 1735 cm^{-1} for cotton and 1737 cm^{-1} for flax can be attributed to C = O stretching of methyl ester and carboxylic acid in pectin and waxes.

Also, the literature mentions that in this FT-IR region the signal of the acetyl group in hemicelluloses occurred (Ouajai et al. 2005). The antisymmetric stretching vibration of the carboxylate group (COO^-) bonded with Ca^{2+} , specific for pectin, appears at approximately 1645 cm^{-1} and overlaps with OH bending of absorbed water which is located between 1500-1700 cm^{-1} (Choe et al. 2018).

On 600 - 1500 cm^{-1} , the specific and common bands for cellulose and hemicellulose were registered. The main infrared vibrations recorded on the above interval are presented in Table 1.

The specific bands for lignin from the lignocellulosic samples were observed at 1278 cm^{-1} and 809 cm^{-1} being given by the G ring and aromatic C-H stretching.

Table 1. Main infrared signals on 600 - 1500 cm^{-1} range for the investigated samples (Dai et al. 2010)

Wavenumber (cm^{-1})	Vibration	Compound
1427	HCH and OCH in-plane bending vibration	Cellulose
1366	In-the-plane CH bending	Cellulose Hemicellulose
1315	CH_2 rocking vibration	Cellulose
1278	C=O and G ring stretching	Lignin
1202	C-O-C symmetric stretching	Cellulose Hemicellulose
1157	C-O-C asymmetrical stretching	Cellulose Hemicellulose
1102, 1052, 1028	C-C, C-OH, C-H ring and side group vibrations	Cellulose Hemicellulose
897	COC, CCO and CCH deformation and stretching	Cellulose
809	C-H vibration	Aromatic hydrogen from lignin
710, 664, 615	OH out-of-phase bending	Cellulose

Quantification of pectin content of samples

Accurate quantification of the remanent pectin content of textile substrates it's the main problem for bioscoured materials characterization when the FT-IR ATR technique is used. Bioscouring

treatments, which aim the elimination of a large amount of pectin from cellulosic and lignocellulosic materials, involve the use of complexing agents such as EDTA or sodium citrate along with mixture of enzymes (pectatylases, pectinlyase, pectinesterases and polygalacturonases).

Due to their specificity, these enzymes act differently on the pectin polymer. For example, pectinesterases act on methyl ester groups while polygalacturonases, pectin lyases and pectatylases depolymerize the pectic chain on which carboxylate groups are bound to Ca^{2+} ions. On the other hand, complexing agents causes the removal of Ca^{2+} from pectin bridges, destabilizes the cell wall structure and facilitates the pectin elimination under the action of enzymes (Kozłowski et al. 2006).

The band absorbance values around 1735 cm^{-1} cannot provide accurate information on the total

amount of pectin from the substrate. The 1735 cm^{-1} FT-IR signal is given only by COOCH_3 and COOH groups in acid form, while the pectin fraction in the form of calcium salts of 1-4-D-polygalacturonic acid cannot be quantified in this wavenumber range. On the other hand, due to the overlap of the OH bending of absorbed water with the COO^- band recorded at $1550\text{ cm}^{-1} - 1700\text{ cm}^{-1}$, the accurate quantification of the pectin content in this wavenumber range is quite difficult. (Dai et al. 2010, Ouajai et al. 2005, Dochia et al. 2018c).

To solve this inconvenience, the investigated samples of cotton and flax raw materials were treated with HCl vapour to convert the carboxylate groups from pectin to acid groups.

Figure 2 presents the FT-IR spectra of cotton and flax raw materials after HCl vapour exposure.

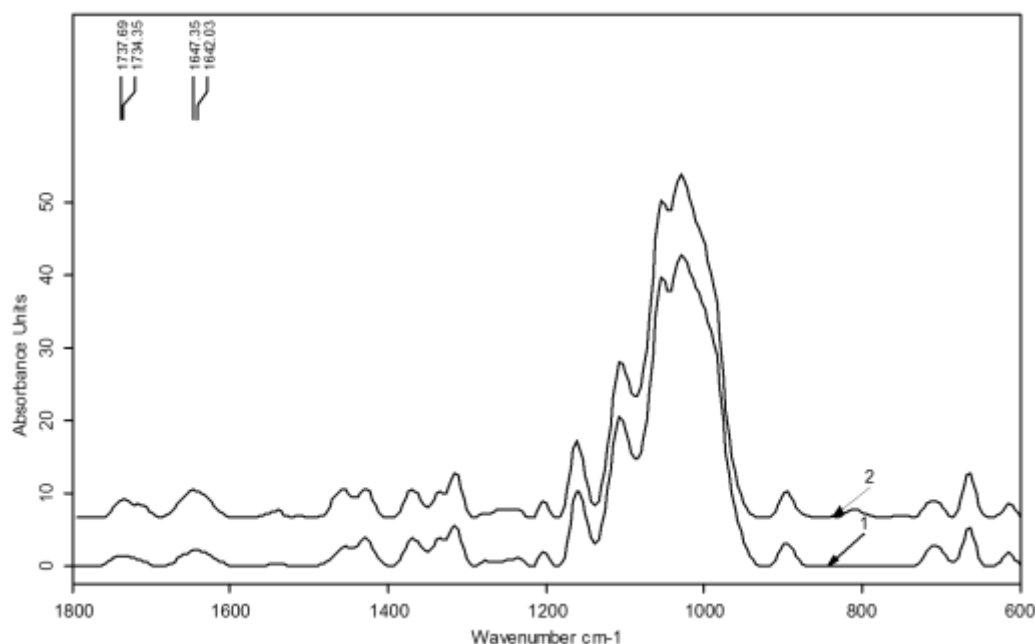


Figure 2. FT-IR ATR spectra of 1- RC and 2 – RF after HCl vapour exposure

Comparing FT-IR spectrum from Figure 2 with Figure 1b, it can be observed an increase in the band intensity located around 1735 cm^{-1} after the exposure of the samples to the action of HCl vapours.

This behaviour can be attributed to the transformation of COO^- groups from polygalacturonic chains into COOH groups.

Table 2 shows the relative absorbance values of the C=O pectin bands from cotton and flax samples before and after HCl vapour exposure.

Table 2. The relative absorbance values of cotton and flax samples before and after HCl vapour exposure

Samples	Wavenumber (cm ⁻¹)	A (a.u.)*
RC - raw	1735	0.75232
RF - raw	1737	1.47179
RC - HCl	1734	2.96447
RF - HCl	1737	4.63010

* The average value of three determinations

The data show that after the treatment with HCl vapours, the values of the relative absorbance of the C = O vibration band of pectin increased approximately 3 times for both types of investigated materials, this being in accordance with data presented in the literature by Choe et. al. (Choe et al. 2018).

As expected, after the exposure of the samples to the action of HCl vapours, a decrease in the relative absorbance value of the ~ 1645 cm⁻¹ band was observed. Thus, in the case of cotton the relative absorbance value decreases from A₁₆₄₅ = 5.18473 (a.u.) to A₁₆₄₂ = 2.22794 (a.u.) and for flax from A₁₆₄₅ = 6.19413 (a.u.) to A₁₆₄₇ = 3.70118 (a.u.). The relative absorbance values from Table 2 confirm higher pectin content in flax samples than in cotton, as was previously presented.

In our opinion, after exposing the samples to the action of HCl vapours, the relative absorbance values of the bands located around 1735 cm⁻¹ allow a more precise quantification of the pectin amount from textile substrates. This procedure can be recommended for an accurate quantification of the amount of remanent pectin in the textile materials subjected to the bioscouring treatment.

CONCLUSIONS

An accurate quantification of pectin content from cotton and flax raw woven fabrics after exposure to HCl vapours was performed by FT-IR ATR analyses. The relative absorbance of pectin-specific bands was evaluated. The results showed an increase in the band intensity values located at ~ 1735 cm⁻¹ and a decrease of the one from ~ 1645 cm⁻¹ after the exposure of the samples to HCl vapours due to the transformation of the (COO⁻) linked with Ca²⁺ groups into acidic carboxylic groups.

Based on the obtained results, this procedure can be useful for the quantification of the remanent pectin from textile substrates after bioscouring treatment.

ACKNOWLEDGEMENTS

This work was supported by a grant of the Romanian National Authority for Scientific Research and Innovation, CNCS-UEFISCDI, project number PN-II-RU-TE-2014-4-1370, and

„Centru de Cercetare în Științe Tehnice și Naturale-CESTN” co-funded by European Union through European Regional Development Fund Structural Operational Program “Increasing of Economic Competitiveness” Priority axis 2. Operation 2.2.1. POSCCE Nr. 621/2014 POS-CCE.

REFERENCES

- Abdel-Halim, E.S., Fahmy, H.M., Fouda Moustafa, M.G., 2008. Bioscouring of linen fabric in comparison with conventional chemical treatment. *Carbohydrate Polymers* 74, 707–711.
- Choe, E. K., Lee, M., Park, K. S., Chung, C., 2018. Characterization of cotton fabric scouring by Fourier transform-infrared attenuated total reflectance spectroscopy, gas chromatography mass spectrometry and water absorption measurements. *Textile Research Journal* 0(00), I - II. DOI:10.1177/0040517518790976journals.sagepub.com/home/trj.
- Ciolacu, D., Ciolacu, F., Popa, V.I., 2011. Amorphous cellulose – structure and characterization. *Cellulose Chemistry and Technology* 45, 13-21.
- Dai, D., Fan, M., 2010. Characteristic and Performance of Elementary Hemp Fibre. *Materials Sciences and Applications* 1, 336-342.
- Dochia, M., Stanescu, M. D., Constantin, C., 2013. Calcium content indicator of scouring efficiency. *Fibres & Textiles in Eastern Europe* 21, 3(99), 22-25.
- Dochia, M., Chambre, D., Gavrilăș, S., Moisă, C., 2018a. Characterization of the complexing agents' influence on bioscouring cotton fabrics by FT-IR and TG/DTG/DTA analysis. *Journal of Thermal Analysis and Calorimetry* 132, 1489–1498.
- Dochia, M., Pustianu, M., Moisă, C., Chambre, D., Gavrilăș, S., 2018b. Sodium citrate as an eco-friendly complexing agent for the bioscouring treatment of the

cellulosic/lignocellulosic fabrics. Chemical Papers 72, 1881–1888.

Dochia, M., Chambre, D., 2018c. Characterization of alkaline and enzymatically treated hemp fibres by FT-IR ATR spectroscopy. Scientific and Technical Bulletin, Series Chemistry, Food Science & Engineering 15(XVI), 18-22.

Eichhorn, S. J., Baillie, C.A., Zafeiropoulos, N., Mwaikambo, L. Y., Ansell, M. P., Dufresne, A., Entwistle, K. M., Herrera-Franco, P. J., Escamilla, G. C., Groom, L., Hughes, M., Hill, C., Rials, T. G., Wild, P. M., 2001. Review-Current international research into cellulosic fibres and composites, Journal of Materials Science, 36, 2107 – 2131.

Jering, A., Gunther, J., Raschka, A., Carus, M., Piotrowski, S., Scholz, L., 2010. Use of renewable raw materials with special emphasis on the chemical industry. ETC/SCP report 1/ 2010, <http://scp.eionet.eu.int>.

Karus, M., Kaup, M., 2002. Natural fibres in the European automotive industry. Journal of Industrial Hemp 7(1), 119-131.

Kozłowski, R., Batog, J., Konczewicz, W., Mackiewicz-Talarczyk, M., Muzyczek, M., Sedelnik, N., 2006. Enzymes in bast fibrous plant processing. Biotechnology Letters 28, 761–765.

Manaia, J.P., Manaia, A.T., Rodrigues, L., 2019. Industrial Hemp Fibers: An Overview. Fibers 7(12), 106-121.

Ouajai, S., Shanks, R.A., 2005. Composition, structure and thermal degradation of hemp cellulose after chemical treatments. Polymer Degradation and Stability 89, 327-335.

Perepelkin, K.E., 2005. Polymeric materials of the future based on renewable plant resources and biotechnologies: fibres, films, plastics. Fibre Chemistry 37, 417-430.

Pursley, D., Lay, L., Maloney, J., Cudd, S., Owens, A., Kerr, J., Sikander, Z., Radvansky, S., 2005. Cotton – the fibre of our web quest, p.14.

Puşcas, E.L., Stănescu, M.D., Fogorasi, M., Dalea, V., 2002. Dezvoltarea durabilă prin protecția mediului și biotehnologii textile, Ed. Universității Aurel Vlaicu Arad, pp. 1-17.

Subramanian, K., Senthil Kumar, P., Jeyapal, P., 2005. Characterization of ligno-cellulosic seed fiber from *Wrightia Tinctoria* plant for textile applications—an exploratory investigation. European Polymer Journal 41, 853–61.

Summerscales, J., Dissanayake, N.P.J., Virk, A.S., Hall, W., 2010. A review of bast fibres and their composites. Part 1 – Fibres as reinforcements. Composite A 41, 1329-1335.

Terpáková, E., Kidalová, L., Eštoková, A., Čigášová, J., Številová, N., 2012. Chemical modification of hemp shives and their characterization. Procedia Engineering 42, 931 – 941.

Wakelyn, P.J., Bertoniere, N.R., French, A.D., Thibodeaux, D.P., Triplett, B.A., Rousselle, M.A., Goynes, W.R., Edwards Jr., J.V., Hunter, L., McAlister, D.D., Gamble, G.R., Cotton Fibers. In: Handbook of Fiber Chemistry. 3th -ed, Menachem L. editors. Taylor & Francis Group, New York, 2007, pp. 523.

Wang, Q., Fan, X., Gao, W., Chen, J., 2006. Characterization of bioscoured cotton fabrics using FTIR ATR spectroscopy and microscopy techniques. Carbohydrate Research 341, 2170–2175.



Open Access

This article is licensed under a Creative Commons Attribution 4.0 International License, which permits use, sharing, adaptation, distribution and reproduction in any medium or format, as long as you give appropriate credit to the original author(s) and the source, provide a link to the Creative Commons license, and indicate if changes were made. The images or other third party material in this article are included in the article's Creative Commons license, unless indicated otherwise in a credit line to the material. If material is not included in the article's Creative Commons license and your intended use is not permitted by statutory regulation or exceeds the permitted use, you will need to obtain permission directly from the copyright holder. To view a copy of this license, visit <http://creativecommons.org/licenses/by/4.0/>.

THE INFLUENCE OF AIR POLLUTANTS ON DIFFERENT MATERIAL USED IN CONSTRUCTION OF MONUMENTS

Alexandru BOGDAN, Lucian COPOLOVICI*

Faculty of Food Engineering, Tourism and Environmental Protection, "Aurel Vlaicu" University, Romania, 2 Elena Dragoi, Arad 310330, Romania

**Corresponding author email: lucian.copolovici@uav.ro*

Abstract: *Urban pollution is one of the most important causes of historical buildings' degradation, thus losing valuable architectural vestiges. This paper presents a literature review concerning the damaging effects of various pollutants on broadly used materials in constructing monuments and buildings, part of the cultural heritage.*

Keywords: air pollution, cultural heritage, atmospheric corrosion

INTRODUCTION

Air pollution prevails to be the main challenge for urban areas and not only when it comes to designing policies that have to meet on the one hand goals regarding traffic efficiency, urban development and on the other hand, to address matters of well-being and conservation of the cultural heritage. Although, many steps of progress have been made in the last decades concerning reducing the level of emission for different pollutants, such as Sulfur dioxide (SO₂), through the advancements in the industry and the heating systems of households – no longer being predominantly based on burning fossil fuels (Grøntoft, et. al., 2019; Patrón, et al., 2017). However, new emerging problems have accelerated the adverse effects of atmospheric pollution.

The poor construction management planning of the recent years in the main urban areas (Arsovski, et al., 2018) and the natural conditions of those regions, for example, wind circulation (Battista & Lieto Vollaro, 2017), generated changes in the quality of living. Traffic emissions continue to be a significant source of harmful pollutants (Vidal, Vicente, & Mendes Silva, 2019) - sulfur dioxide (SO₂), nitrogen dioxide (NO₂), particulate matter (PM), causing premature deaths (Arsovski, et al., 2018) and having an extensive role in the degradation of materials used in construction, notably in the case of buildings part of the cultural heritage (Christodoulakis, et al., 2017).

Modification in climatic factors, such as rainfall; wind circulation; temperature variations - caused by the increasing levels of pollution and the adverse effects of climate

change (Christodoulakis, Tzani, Varotsos, Ferm, & Tidblad, 2017; Vidal, Vicente, & Mendes Silva, 2019), lead to the accelerated destruction of the monuments and buildings included in those area's cultural heritage. These processes could have irreversible adverse effects not only on the aspect of individual cities but also on the general view of a country, as many times the aesthetic of a country's building heritage is associated with its global image (Arsovski, et al., 2018; Patrón, et al., 2017).

The primary atmospheric pollutants causing material degradation of building heritage are sulfur dioxide (SO₂), nitrogen dioxide (NO₂), and particulate matter (PM). Sulfur dioxide (SO₂) is emitted through the combustion of sulfur-containing fuels. In contrast, nitrogen dioxide (NO₂) is formed mainly by the oxidation of nitrogen monoxide (NO) after combustion processes which take place at high temperatures (Benga, 2019; Boamfã, et al., 2018). Particulate matter (PM) is the generic term used for a mixture of aerosol particles (solids and liquids), with different sizes and chemical compositions. PM can come from natural sources: sea salt; suspended dust; pollen; volcanic ash or anthropogenic sources, especially from the burning of fuels for the production of heat and electricity (Benga, 2019; Vidal, et al., 2019).

This paper aims to present an opinion concerning the damaging effects of various pollutants on broadly used materials in constructing monuments and buildings, part of the cultural heritage.

The influence of pollutants on metals

The main damaging effect of pollutants on metal objects or surfaces of heritage buildings and monuments is corrosion due to environmental conditions (Vidal, et al., 2019). Corrosion is an irreversible electrochemical reaction between the metal and the compounds present in the environment, which leads to the modification of the metal or the initial alloy (Benga, 2019). These processes affect the overall aesthetics of the specific surface and decrease the metal's mechanical properties (Vidal, et al., 2019).

The presence of an electrolyte induces a corrosive reaction. Therefore, the exposure of the metal objects to wetness, due to condensed humidity (Vidal, et al., 2019), as a result of rainfalls, depending on their acidity, or thermal inversions (Patrón, et al., 2017), could be the main damaging factor of monuments and sculptures made by metal. In a study focusing on the impact of air pollution in Athens, the authors underline, also based on previous studies, that carbon steel is affected the most by corrosion processes (Christodoulakis, et al., 2017). Additionally, studies mapping pollutants impact in Mexico has demonstrated that degradation of its building heritage is mainly caused by acid rains (Castillo-Miranda, et al., 2017).

The influence of pollutants on glass

Atmospheric weather pollution is one of the main phenomena affecting glass surfaces. These processes can alter the glass's clarity, resulting in decreasing natural light levels and affecting the overall aesthetics of the building itself (Vidal et al., 2019).

Reversing soiling processes could represent a costly challenge to preserve glass surfaces. Soiling is connected with atmospheric pollution, being an easily noticeable effect of traffic emissions and acidic rainfalls. Grøntoft et al. (2019) present the cleaning costs of sheltered white painted steel and modern glass in their study. Reducing pollution levels could also reduce the amount of European money city administrations spend on cleaning due to air pollution.

The influence of pollutants on limestone, stone, marble

As in the case of metal objects and surfaces, in the case of limestone; stone and marble surfaces of buildings part of the cultural heritage, exposure to different environmental processes, such as acid rain; temperature variations, or acid depositions (Vidal et al., 2019) could cause irreversible aesthetic and structural damages.

The severity of the building's degradation effects depends mainly on the percentage these stone materials take up in the specific facility's entire surface (Lefevre, et al., 2016). The more porous is the stone material used for the construction, the more water it will take in, leading to the dissolution of carbonate minerals, gypsum formation, and in the most severe cases, even cracking (Castillo-Miranda, et al., 2017; Ortega-Morales, et al., 2019). Studies concerning pollutants impact on stone materials were conducted mostly in Europe, focusing on cases such as the one of the St. Rumbold's Cathedral in Mechelen, Belgium, where the erosion of its limestone surfaces was linked to gypsum formation (Castillo-Miranda, et al., 2017).

Several other processes regarding pollution can influence the appearance of stone surfaces. For example, surface deposits on stone, such as dust, black crusts, and soiling in general, are the ones that decrease the most of the aesthetic of these materials, ultimately also their resistance in time. However, the monitoring of these processes could improve the understanding of certain changes in pollution levels in a specific area (Ortega-Morales, et al., 2019; Patrón, et al., 2017) contribute to the implementation of more well-thought urban management programs.

The influence of pollutants on concrete and mortars

Carbonation is the most extensively studied influence of pollutants on concrete and mortars, as this process implies a chemical reaction between the atmospheric CO₂ and the cement products. This process reduces the cement's pH and leaves the surfaces without protection in corrosion (Vidal, 2019). When the layer of concrete weakens, it will undermine the building's structural resistance and lead to cracking and detaching. Thermal variations and

increased humidity, especially in valleys, can affect the concrete and mortar surface through volume contractions (Ortega-Morales, et al., 2019).

Conclusions

The decrease in coal use as a primary heating source leads to significant improvements in air quality and pollution tackling processes. However, global climate change (Patrón, et al., 2017) and other pollutants represent still a challenge to ensure the well-being and preserve cultural heritage.

The influence of pollutants on the different materials used for the construction of buildings, part of the cultural heritage, is a matter which impacts not only the structural resistance of these buildings but also the aesthetics of those areas, with lasting effects on living conditions and tourism.

REFERENCES

Arsovski, S., Kwiatkowski, M., Lewandowska, A., Jordanova Peshevska, D., Sofeska, E., & Dymitrow, M. 2018. Can urban environmental problems be overcome? The case of Skopje—world's most polluted city. *Bulletin of Geography. Socio-economic Series*, 17-39.

Battista, G., & Lieto Vollaro, R. d. 2017. Correlation between air pollution and weather data in urban areas: Assessment of the city of Rome (Italy) as spatially and temporally independent regarding pollutants. *Atmospheric Environment*, 240-247.

Benga, I.-C. 2019. *Calitatea Aerului Ambiental în aglomerarea Braşov. Raport pentru anul 2019*. Braşov: Agenția pentru Protecția Mediului Braşov.

Boamfă, M.-I., Jiman, O., Milin, V., Popa, L., & Mureşan, A. (2018). *Studiu privind calitatea aerului în Municipiul Braşov*. Braşov: Primăria Municipiului Braşov.

Castillo-Miranda, J., Torres-Jardón, R., Garcia-Reynoso, J., Mar-Morales, B., Rodríguez-Gómez, F., & Ruiz-Suarez, L. 2017. Mapping recession risk for cultural heritage stone in Mexico City due to dry and wet deposition of urban air pollutants. *Atmósfera*, 189-207.

Christodoulakis, J., Tzanis, C., Varotsos, C., Ferm, M., & Tidblad, J. 2017. Impacts of air pollution and

climate on materials in Athens, Greece. *Atmospheric Chemistry and Physics*, 439-448.

Grøntoft, T., Verney-Carron, A., & Tidblad, J. 2019. Cleaning costs for European sheltered white painted steel and modern glass surfaces due to air pollution since the year 2000. *Atmosphere*, 1-31.

Lefe'vre, R.-A., Ionescu, A., Desplat, J., Kounkou-Arnaud, R., Perrussel, O., & Languille, B. 2016. Quantification and mapping of the impact of the recent air pollution abatement on limestone and window glass in Paris. *Environ Earth Sci*, 1-12.

Ortega-Morales, O., Montero-Muñoz, J., Baptista Neto, J., Beech, I., Sunner, J., & Gaylarde, C. 2019. Deterioration and microbial colonization of cultural heritage stone buildings in polluted and unpolluted tropical and subtropical climates: A meta-analysis. *International Biodeterioration & Biodegradation*, 1-11.

Patrón, D., Lyamani, H., Titos, G., Casquero-Vera, J., Cardell, C., Mocnik, G., Olmo, F. 2017. Monumental heritage exposure to urban black carbon pollution. *Atmospheric Environment*, 22-32.

Vidal, F., Vicente, R., & Mendes Silva, J. (2019). Review of environmental and air pollution impacts on built heritage: 10 questions on corrosion and soiling effects for urban intervention. *Journal of Cultural Heritage*, 273-295.

Wang, X.J., Zhang, L.L., Yao, Z.J., Ai, S.Q., Qian, Z.M., Wang, H., 2018. Ambient coarse particulate pollution and mortality in three Chinese cities: Association and attributable mortality burden. *Science of the Total Environment* 628-629, 1037-1042.



Open Access

This article is licensed under a Creative Commons Attribution 4.0 International License, which permits use, sharing, adaptation, distribution and reproduction in any medium or format, as long as you give appropriate credit to the original author(s) and the source, provide a link to the Creative Commons license, and indicate if changes were made. The images or other third party material in this article are included in the article's Creative Commons license, unless indicated otherwise in a credit line to the material. If material is not included in the article's Creative Commons license and your intended use is not permitted by statutory regulation or exceeds the permitted use, you will need to obtain permission directly from the copyright holder.

To view a copy of this license, visit <http://creativecommons.org/licenses/by/4.0/>.

THE INFLUENCE OF GRAPEVINE PRUNING ON THE LEVEL CROP AND QUALITY IN CABERNET SAUVIGNON CLONES

Constantin BADUCA¹, Felicia STOICA¹, Camelia MUNTEAN¹

¹Faculty of Horticulture, University of Craiova, Romania, 13 A.I. Cuza, Craiova, 220585, Romania
Corresponding author email: cbaduca@gmail.com, feliciastoica@yahoo.com,
camelia_muntean@hotmail.com

Abstract: Yield is one of the factors with major influence on the quality of grapevine production. Winter pruning is the first way to control yield. In this study we applied 3 cutting variants to 4 clones of Cabernet Sauvignon from Sâmburești vineyard, one of the most famous Romanian vineyards for quality red wines. The results of the study show that in order to obtain the typical Cabernet Sauvignon wines in the Sâmburești vineyard, winter pruning is recommended with a maximum of 9 nodes/m² or a delay in harvesting until more advanced stages of maturity compared to what we applied in this study.

Keywords: red wine, pruning, clones.

INTRODUCTION

Crop yield is widely recognized as an important factor in the quality of resultant wines, but most prior research has shown no effect of yield on wine quality (Chapman D. et al., 2004). Grapevine yield and fruit composition largely depend on vine water status, which can be manipulated, especially in semiarid climates, by irrigation strategies and training systems (Mirás-Avalos J. et. al., 2017). Each training system involves specific grapegrowing conditions, which affect the concentration of volatile metabolites of grape (Mariagiovanna Fragasso M. et al., 2012).

The potential yield of grapevines is often inexpensively manipulated by altering the number of nodes retained per vine after pruning (Greven M.M. et. al., 2014). Minimal pruning (MP) is a technique used to reduce labor costs and produce high-quality winegrapes (Zheng W. et. al., 2017). Bunch number per node or shoot varies significantly between seasons and is a major cause of yield variation. Varying total node numbers by pruning is the least expensive way to regulate yield. However, there is little information available on how varying bearer length (and thus node number) in a machine-pruned canopy alters yield components (McLoughlin S.J. et. al., 2011).

Viticultural practices are highly influential in berry and wine composition. The effects of crop-level reduction on berry composition are normally an increase in soluble solids (Brix) and a concomitant increase in ethanol in the wine produced (Morena Luna

L.H. et. al., 2018). Environmental factors such as light and field management practices have a combined effect on grapevine physiology and wine quality (Feng, H. et al., 2017).

Seasonal fluctuations in yield, grape composition and wine attributes, largely driven by variable climatic conditions, are major challenges for the wine industry aiming to meet consumer expectations for consistent supply, wine style and product quality (Clingeffer P.R., 2010). Pruning during winter when grapevines are dormant is an important cultural operation grapegrowers use to regulate yield. Pruning is a relatively simple and straightforward method that can be used to directly select the type of buds retained, as well as limit the number of buds per vine (Martin, S. R., Dunn G. M., 2000). Vines can be pruned leaving either a predominance of long canes (cane pruning) or short spurs (spur pruning) on a perennial "cordon" structure. Despite some well documented advantages of spur pruning including more uniform shoot growth and higher capacity for the storage of reserves (Bernizzoni et al., 2009).

MATERIALS AND METHODS

4 clones of Cabernet Sauvignon from the Sâmburești vineyard assortment were studied: 169, 337, 338, 685, all grafted on the rootstock SO4, in identical climate and soil conditions, in the year 2019. The plantation was established in 2010, with planting distances of 2.25 m between rows and 1 m per row, which means a density of

4545 vines/ha, and the training system was identical (Guyot).

3 pruning variants were applied, respectively three loads of eyes on the stem after the winter pruning, 9, 12, 15 nodes/m², which means 20, 27 and 34 nodes/vine. For each experimental variant, 10 consecutive vines in the same row were studied.

The production from each vine was weighed and put in bags on each variant. The bags were transported to the University of Craiova, Faculty of Horticulture, Oenology Laboratory for analysis. The following were determined: the average weight of the bunches, the production per vine and per hectare, calculated by multiplying the average weight of the grapes by the average number of grapes per vine, the sugar content (g/L) by densimetric method and the total acidity (g/L acid tartaric acid) by titration with 0.1 N NaOH solution.

RESULTS AND DISCUSSIONS

As the number of nodes left on the vine after the winter pruning increases, the number of grapes on the vine increases, but the increases are uneven between variants (table 1). Thus, for the most severe pruning, which leaves only 9 nodes/m² (which means 20 nodes/vine), the number of grapes harvested varies between 12 (per clone 169) and 15 (clones 338 and 685). Therefore, in all 4 clones, the number of grapes harvested was lower than the number of nodes left on the vine after winter pruning. This must be linked to several factors that did not result in a fertile shoot from each node left on the vine. The causes can be multiple, including low spring temperatures after budburst.

For medium severity pruning (12 nodes/m²), equivalent to 27 nodes/vine, the number of grapes varied between 15 (clone 169) and 22 (clone 685) and for the longest pruning (15 nodes/m², equivalent to 34 nodes/vine), the number of grapes was between 18 (clone 169) and 26 (clone 685). Therefore, for all pruning options, clone 169 had the lowest and clone 685 had the highest number of grapes.

In all pruning variants, the increase in the number of grapes per vine is accompanied by a decrease in their average weight.

At the cutting variant with 9 nodes/m² the average weight of the grapes varies between

126.1 g (clone 685) and 185.1 g (clone 169). In the 12 nodes/m² pruning variant, the average weight of the grapes varies between 119.2 g (clone 685) and 177.7 g (clone 169). In the 15 nodes/m² pruning variant, the average weight of the grapes varies between 111.5 g (clone 685) and 168.5 g (clone 169). Clone 337 showed the largest decrease in average grape weight of 12 g from severe to medium pruning, while clone 685 showed the smallest decrease in average grape weight (7 g) between the two cutting variants. Between the medium (12 nodes/m²) and light (15 nodes/m²) pruning variants, the largest decrease in the average weight of the grapes was 11.6 g and was also in clone 337 but the smallest decrease was of 3.9 g and was recorded in clone 338.

Table 1. Number of bunches/vines and average weight of grapes

Pruning variant	Bunches/vine	Average weight grapes (g)
Clone 169, 9 nodes/m ²	12	185.1
Clone 169, 12 nodes/m ²	15	177.7
Clone 169, 15 nodes/m ²	18	168.5
Clone 337, 9 nodes/m ²	13	142.0
Clone 337, 12 nodes/m ²	16	130.1
Clone 337, 15 nodes/m ²	20	119.5
Clone 338, 9 nodes/m ²	15	129.8
Clone 338, 12 nodes/m ²	20	119.6
Clone 338, 15 nodes/m ²	25	115.7
Clone 685, 9 nodes/m ²	15	126.1
Clone 685, 12 nodes/m ²	22	119.2
Clone 685, 15 nodes/m ²	26	111.5

The production of grapes per stem varied between 1.85 kg (clones 337, 9 nodes/m²) and 3.03 kg (clones 169, 15 nodes/m²) and the production per hectare varied between 8,390 and 13,784 kg. In the cutting variant with 9 nodes/m² only one clone had the production over 2 kg/vine (clone 169, with 2.22 kg), the other 3 clones having m yields less than 2 kg/vine: clone 337 (1.85 kg), clone 685 (1.89 kg) and clone 338 (1.94 kg). In fact, the 337 clone had the lowest yields of all cutting variants. At the cutting variant with 15 nodes/m², clone 169 was noted, the only one with a production higher than 3 kg/ha and with 13,784 kg / ha. Two other clones (338 and 685) had yields over 13,000 kg/ha, only clone 337 had less than 13,000 kg/ha in the cutting variant with 15 13,784 nodes/m² (table 2).

Table 2. Grape production

Pruning variant	Yield kg/vine	Yield kg/ha
Clone 169, 9 nodes/m ²	2.22	10,095
Clone 169, 12 nodes/m ²	2.66	12,114
Clone 169, 15 nodes/m ²	3.03	13,784
Clone 337, 9 nodes/m ²	1.85	8,390
Clone 337, 12 nodes/m ²	2.08	9,460
Clone 337, 15 nodes/m ²	2.39	10,862
Clone 338, 9 nodes/m ²	1.94	8,849
Clone 338, 12 nodes/m ²	2.41	10,944
Clone 338, 15 nodes/m ²	2.89	13,146
Clone 685, 9 nodes/m ²	1.89	8,596
Clone 685, 12 nodes/m ²	2.62	11,918
Clone 685, 15 nodes/m ²	2.90	13,175

The values of the main grape composition parameters (sugars and total acidity) were significantly influenced by the production levels resulting from the application of different pruning variants. The most important finding from the analysis of data on the chemical composition of grapes is that in all clones, as the yield increases, the sugar content decreases.

Table 3. Sugars content and titratable acidity of grapes at harvest

Pruning variant	Sugars, g/L	Total acidity, g/L tartaric acid
Clone 169, 9 nodes/m ²	228	4.10
Clone 169, 12 nodes/m ²	210	4.22
Clone 169, 15 nodes/m ²	192	4.85
Clone 337, 9 nodes/m ²	236	4.00
Clone 337, 12 nodes/m ²	212	4.52
Clone 337, 15 nodes/m ²	198	4.95
Clone 338, 9 nodes/m ²	232	4.12
Clone 338, 12 nodes/m ²	208	4.48
Clone 338, 15 nodes/m ²	195	5.10
Clone 685, 9 nodes/m ²	224	4.16
Clone 685, 12 nodes/m ²	204	4.78
Clone 685, 15 nodes/m ²	190	5.20

In the 9 nodes/m² cutting variant, the sugar content varied between 224 g/L (clone 685) and 236 g/L (clone 337), in the medium cutting variant the sugar contents varied between 204 g/L (clone 685) and 212 g/L (clone 337) and at the cutting variant with 15 nodes/m² the sugar contents varied between 190 g/L (clone 685) and 198 g/L (clone 337). Therefore, of all the cutting variants, clone 685 had the lowest, while clone 337 had the highest sugar

content. The data in Table 3 also show that in the 15 nodes/m² cutting variant the sugar contents were below 200 g/L in all clones, which shows that this cutting variant is not suitable for obtaining quality wines.

The total acidity of the grapes increased as the grape production increased, contrary to the sugar content. The lowest total acidity was 4 g/L tartaric acid (clones 337, 9 nodes/m²), and the highest was 5.20 g/L tartaric acid (clones 685, 15 nodes/m²).

CONCLUSIONS

There was a strong link between the fruit load after winter pruning and the number of grapes per vine, but there was no directly proportional relationship between the increase in the number of nodes and the increase in the number of grapes per vine. This is due to the fact that the nodes left on the vine after cutting is one of the main factors on which grape production depends, but it is not the only one, along with other factors of a technological or ecological nature. In all variants, the increase in the number of grapes per vine was accompanied by a decrease in their average mass in absolutely all cases. Even if the increase in the number of grapes on the stalk was accompanied by a decrease in their mass, the production of the vine increased as the fruit load increased.

The increase in yield has not proved to be conducive to increasing the quality of wine production. In the present study we took into account only the sugar contents and total acidity of the grapes at the time of harvest (so-called technological maturity). For this reason, the maximum fruit load, of 15 nodes/m², which led to very high yields, led to sugar contents below 200 g/L, even dropping to 190 g/L. From such sugar contents are obtained wines with moderate alcoholic strengths of 11-12% vol., much of which is characteristic of quality wines obtained in the Sâmburești vineyard. Also, the cutting variants with a fruit load of 12 nodes/m², have sugar contents of 204-212 g/L, also unsuitable for obtaining strong, rich, structured, generous Sâmburești wines, as recognized by informed consumers of quality wines from our country and how they are recognized on the domestic and international market of quality wines.

REFERENCES

1. Bernizzoni, F., Gatti, M., Civardi, S., Poni, S., 2009, Long-term performance of Barbera grown under different training systems and within-row vine spacings. *American Journal of Enology and Viticulture*, vol. 60, issue 4, pp. 339-348.
2. Chapman, D., Matthews, M., Guinard, J.X., 2004, Sensory Attributes of Cabernet Sauvignon Wines Made from Vines with Different Crop Yields. *American Journal of Enology and Viticulture*, vol. 55, issue 4, pp. 325-334.
3. Clingeffer, P.R., 2010, Plant management research: status and what it can offer to address challenges and limitations. *Australian Journal of Grape and Wine Research*, vol. 16, Special issue, pag. 25–32.
4. Feng, H., Skinkis, P.A., Qian, M.C., 2017, Pinot noir wine volatile and anthocyanin composition under different levels of vine fruit zone leaf removal. *Food Chem.* 214, 736-744.
5. Greven, M.M., Bennett J.S., Neal, S.M., 2014. Influence of retained node number on Sauvignon Blanc grapevine vegetative growth and yield. *Australian Journal of Grape and Wine Research*, vol. 20, Issue 2, pp. 263-271.
6. Mariagiovanna Fragasso, M., Antonacci, D., Pati, S., Tufariello, M., Baiano, M., Forleo L., Caputo, A., La Notte, E., 2012. Influence of Training System on Volatile and Sensory Profiles of Primitivo Grapes and Wines. *American Journal of Enology and Viticulture*, vol. 63, issue 4, pp. 477-486.
7. Martin, S. R. Dunn, G. M. 2000, Effect of pruning time and hydrogen cyanamide on budburst and subsequent phenology of *Vitis vinifera* L. variety Cabernet Sauvignon in central Victoria. *Australian Journal of Grape and Wine Research*, vol. 6, issue 1, pp. 31-39.
8. Mirás-Avalos, J., Buesa, I., Llacer, Elena, Jiménez-Bello, M., Risco, D., Castel, J., Intrigliolo D., 2017. Water Versus Source–Sink Relationships in a Semiarid Tempranillo Vineyard: Vine Performance and Fruit Composition. *American Journal of Enology and Viticulture*, vol. 68, issue 1, pp. 11-22.
9. McLoughlin, S.J., Petrie, P.R., Dry, P.R., 2011, Impact of node position and bearer length on the yield components in mechanically pruned Cabernet Sauvignon (*Vitis vinifera* L.). *Australian Journal of Grape and Wine Research*, vol. 17, issue. 2, pp. 129–135.
10. Morena Lunam, L.H., Reynolds, A.G., di Profio, F.A., Zhang, L., Kotsaki, E., 2018, Crop Level and Harvest Date Impact on Four Ontario Wine Grape Cultivars. II. Wine Aroma Compounds and Sensory Analysis. *South African Journal of Enology and Viticulture*, Vol. 39, issue 2, pp. 246-270.
11. Zheng, W., del Galdo, V., García, J., Balda, P., Martínez de Toda, F., 2017, Use of Minimal Pruning to Delay Fruit Maturity and Improve Berry Composition under Climate Change. *American Journal of Enology and Viticulture*, vol. 68, issue 1, pp. 136-140.



Open Access

This article is licensed under a Creative Commons Attribution 4.0 International License, which permits use, sharing, adaptation, distribution and reproduction in any medium or format, as long as you give appropriate credit to the original author(s) and the source, provide a link to the Creative Commons license, and indicate if changes were made. The images or other third party material in this article are included in the article's Creative Commons license, unless indicated otherwise in a credit line to the material. If material is not included in the article's Creative Commons license and your intended use is not permitted by statutory regulation or exceeds the permitted use, you will need to obtain permission directly from the copyright holder.

To view a copy of this license, visit <http://creativecommons.org/licenses/by/4.0/>.

ZR(IV) MOFS BASED ON TEREPHTHALIC ACID AND ACETIC ACID MODULATOR

Mirela PICIORUS, Alexandru POPA, Catalin IANASI, Elisabeta I. SZERB, Carmen CRETU*

“Coriolan Dragulescu” Institute of Chemistry, Romanian Academy, 24 Mihai Viteazu Bvd.,
300223 Timisoara, Romania

Corresponding author email: carmencretu78@gmail.com

Abstract: Herein, we present the investigation of a fast modulated synthesis of micro/meso sized ZrMOF, porous materials known as UIO-66, containing terephthalic acid (H_2BDC) as organic linker using an excess of metal salt precursor and different concentrations of acetic acid (AAc) as organic modulator. The increase in the concentration of modulator up to a certain value leads to an improvement of surface area and a modification of pore structure by producing mesopores at the expense of micropores.

Keywords: Zirconium (IV) Metal-organic frameworks; terephthalic acid; surface area

INTRODUCTION

Metal-organic frameworks (MOFs) are an innovative class of crystalline porous materials constructed from metal nodes or clusters coordinated by organic linkers into two-dimensional or three-dimensional extended periodic network structures (Chen et al. 2019, Sharmin et al. 2016). These compounds have attracted much interest in recent years, due to i) their structural and topological characteristics and ii) for large area of applications based on their large internal surface area, permanent porosities, tunable pores, as well as their versatile functionalities (Li et al. 2016, Fang et al. 2018). Different combinations of metals and organic binders may provide an infinite number of MOFs structures with distinct physico-chemical properties (Bai et al. 2016). The type of metal centre (ion radius, coordination number, electron configuration), interaction/ distances between the metal ions, the coordination ability of the ligand and the ligand shape (bend, length, and substituents) controls the entire structure topology (Xiong et al. 2016). Different types of carboxylate ligands, flexible and rigid ones, are employed in the construction of MOFs (Wang et al. 2015), though the aromatic rigid dicarboxylate ligands have been extensively used due to the stability and permanent porosity of the resulting materials (Angeli et al. 2020). Other factors with relevance in the MOFs architecture are metal-to-ligand molar ratios, solvent and reaction temperatures,

counter ions and pH values of the reaction systems, etc (Seetharaj et al. 2019, Yao et al. 2019, Li et al. 2017, Winarta et al. 2020).

ZrMOFs are one of the most studied porous materials based on their high porosity, exceptional thermal, structural and water stability, with versatile potential applications, including gas storage (Ghanbari et al. 2020), molecule adsorption (Chang et al. 2020, Guan et al. 2020), catalysis (Su et al. 2020, Kirlikovali et al. 2020), drug delivery (Jiang et al. 2019), luminescence biosensing (Liu et al. 2020), molecular recognition (Wang et al. 2019) and so on. The enhanced stability of ZrMOFs can be attributed to the strength of the Zr-O coordination bonds caused by acid-hard base interactions between Zr (IV) atoms and oxygen atoms (Drout et al. 2019). The first ZrMOFs (UIO-66 series) based on terephthalic acid derivative were reported by Cavka and collaborators (Cavka et al. 2008), wherein $Zr_6O_4(OH)_4$ octahedral secondary building units (SBUs) link twelve linear dicarboxylate linkers, each in three dimensions to form a highly porous structure and high structural resistance against water and external mechanical pressure (Kalaj et al. 2020, Han et al. 2018). The obtaining of large single crystal or compact polycrystalline films are hard to achieve. Thus, in this direction, numerous studies have been showed that the inclusion of monocarboxylic acids as modulators, into the synthesis of zirconium MOFs can help the crystallization of the final product (Feng et al. 2015) by slowing down

the crystal formation or can affect it turning in a gel-like amorphous product (Hu et al. 2015). Schaate et al. (Schaate et al. 2011) have shown the importance of choosing of a proper type and amount of modulator and maintaining an equilibrium exchange between the modulator and dicarboxylic acid used in order to control the crystallite and particle sizes of the product. Moreover, the modulator or the linker can promote the formation of defects in the MOF structure, followed by an increase in the surface area and pore volume (Helal et al. 2020) with a positive impact in applications such as gas adsorption and catalysis (Taddei 2017, Ren et al. 2017)

Since the MOF architecture is greatly dependent on the metal-to-ligand molar ratios and the majority of the studies are based on a 1 to 1 molar ratio, we chose to investigate the modulator influence in metal precursor excess synthesis condition respectively in a 1.5 to 1 metal-to-ligand ratio. Accordingly, herein we report the investigation of a fast modulated synthesis of micro/meso sized ZrMOF porous materials containing terephthalic acid as organic linker, excess of Zr salt precursor and different concentration of acetic acid (AAc) as organic modulator.

MATERIALS AND METHODS

All commercially available reagents and solvents were of analytical grade and used without further purification. Zirconium oxychloride octahydrate ($\text{ZrOCl}_2 \cdot 8\text{H}_2\text{O}$), N,N-dimethylformamide (DMF) were purchased from Riedel de Haën, terephthalic acid (H_2BDC) and ethanol (EtOH) were from Sigma Aldrich, and acetic acid (CH_3COOH) was purchased from Silal Trading. Infrared spectra (KBr) in the range $4000\text{--}400\text{ cm}^{-1}$ were recorded on a Cary 630 FT-IR spectrophotometer. Thermal analysis curves were obtained in the temperature range of $25\text{--}800\text{ }^\circ\text{C}$ (heating rate of $10\text{ }^\circ\text{C}/\text{min}$) using a TGA/SDTA 851/LF/1100 Mettler Toledo thermo-gravimetric analyzer. The experiments were conducted under a nitrogen flow of $50\text{ mL}/\text{min}$ and dynamic atmosphere of air introduced at $800\text{ }^\circ\text{C}$ followed by a final isothermal heating for 15 min. The samples with mass of about $10\text{--}20\text{ mg}$ were placed in

alumina crucible of 150 mL. The textural parameters were obtained by using Surface Area & Pore Size Analyzer Quantachrome Nova 1200e apparatus. In order to prepare the material for analysis, the samples were degassed under vacuum for 17 h at 100°C . The N_2 adsorption-desorption isotherms were acquired using 44 point in the 0.05-1 P/Po interval at 77K. Using a NovaWin software, the surface area was determined using BET (Brunauer, Emmett, Teller) (Brunauer et al. 1938) and the total pore volume was determined from the last point which is closest to 1P/Po. The pore size distribution (PSD) was determined by DFT method using the calculation model: N_2 at 77 K on carbon for slit pore with NL-DFT (Non-Local Density-functional theory) equilibrium model (Ravikovitch et al. 1995). This method is specific for microporosity not just mesoporosity.

Synthesis

The synthesis of zirconium-dicarboxylate MOFs noted as ZrMOF_equivalents of acetic acid, was based on a previously reported procedure with some amendments (Chen et al. 2018). ZrMOFs were prepared *in a closed bottom flask* by heating solutions containing zirconium salts as precursor, terephthalic acid as ligand, and acetic acid as a modulator.

General method: Terephthalic acid (400 mg, 2.4 mmol), $\text{ZrOCl}_2 \cdot 8\text{H}_2\text{O}$ (1150 mg, 3.5 mmol), acetic acid (amounts of AAc: 0 mL for ZrMOF_0eq; 2.65 mL, 46 mmol for ZrMOF_13eq; 5.3 mL, 92 mmol for ZrMOF_26eq; 10.6 mL, 185 mmol for ZrMOF_52eq; 21.2 mL, 370 mmol for ZrMOF_104eq), DMF (18 mL) were combined in a 50 mL borosilicate glass, sealed and heated to 120°C for 24 h. The solution was cooled at room temperature. The white polycrystalline powders were collected by filtration and air dried. As-synthesized samples were washed with 10 mL of DMF two times/day during three days and immersed in ethanol, followed the same procedure as washing in DMF. The solid was then dried at 160°C under vacuum for 12 h to yield activated sample.

RESULTS AND DISCUSSIONS

All ZrMOFs reported here were obtained keeping constant the solvent volume and the molar ratio between terephthalic acid and zirconium salt (1:1.5) and increasing the amount of AAC from 0 to 104 molar equivalents. Similar studies were reported on ZrMOFs based on terephthalic (UIO-66) using different metal-ligand molar ratio and various types/amount of modulator (Li et al. 2016, Schaate et al. 2011, Han et al. 2015).

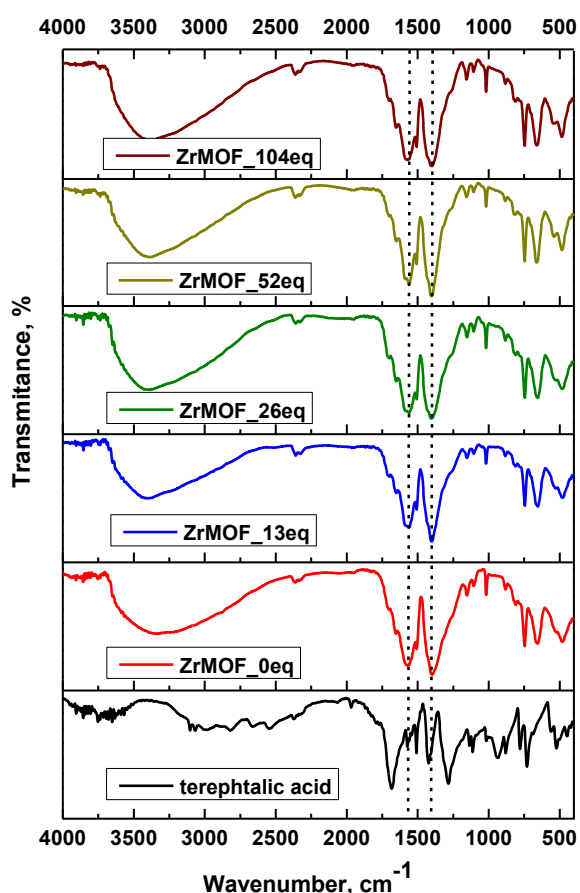


Figure 1. FT-IR spectra of the ZrMOFs samples with different amount of AAC vacuum dried at 160°C.

The FT-IR spectra of the samples (Figure 1) reveal the presence of coordinated carboxylate groups by the asymmetric and symmetric stretching vibrations found around 1580 cm^{-1} and 1400 cm^{-1} , respectively (Yang et al. 2018) when compared with the free ligand presenting only one band at 1680 cm^{-1} . The bands around 1660 cm^{-1} observed in all samples can be attributed to the stretching modes of the carbonyl group (C=O) of the DMF residues trapped inside the pores (Winarta et al. 2020). The bands in the range 1156-1100 cm^{-1} and 781-482 cm^{-1} are

assigned to the C-H in-plan and out-of-plane ring bending, respectively (Silverstein et al. 1998). The bands found in the range 661-653 cm^{-1} are attributed to asymmetric vibration of the Zr-(μ_3 -O) bridges in the framework building blocks (Piszczek et al. 2007) and the band around 500 cm^{-1} is associated with the stretching vibration of Zr-(OC) bonds (Wang et al. 2017).

The thermal decomposition of the activated ZrMOFs was investigated in dynamic nitrogen atmosphere from ambient temperature to 800°C when air dynamic atmosphere was introduced followed by an isothermal heating for 15 minutes (Figure 2).

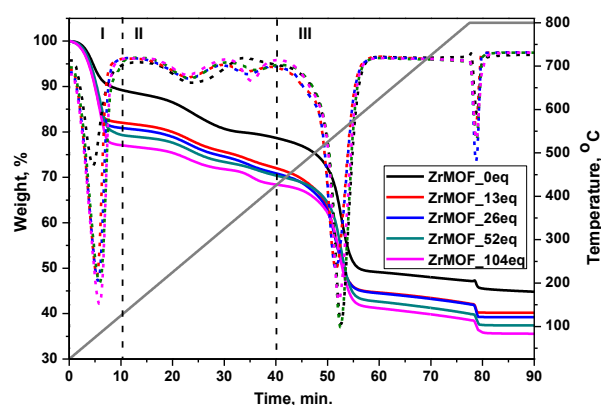


Figure 2. TGA (solid line) and DTG (short dash line) curves of the activated ZrMOFs.

All samples have been vacuum dried at 160°C; however, they are highly hygroscopic when kept in air atmosphere. The TG/DTG curves revealed three important weight loss steps highlighted on DTG curve by intense and well delimited peaks (first and third steps) and broad peaks (second step) (Table 1). The first step in the curve was in the range of temperature from 25°C to 150°C and can be attributed to the loss of the physisorbed water. The weight loss of water increases from the free acetic acid sample to the sample with highest content of modulator as follows: 11,58% (ZrMOF_0eq) < 18,29% (ZrMOF_13eq) < 19,44% (ZrMOF_26eq) < 21,06% (ZrMOF_52eq) < 23,35% (ZrMOF_104eq). The increased capacity to retain water can be explained by the changes of the porous structure and surface area (Pan et al. 1996). The second step, up to 420°C, contain two not well resolved weight losses associated with the dehydroxylation of the

metal node (ca. 150-330°C), and removal of acetic acid (ca. 330-420°C) (Ardila-Suarez et al. 2019). In the third step, starting with 420°C the decomposition of the linker (terephthalic acid) took place, followed by the obtaining of ZrO₂ residue, after complete degradation of the organic moiety at 800°C.

Table 1. Temperature of decomposition stages on DTG tomograms and the content of ZrO₂

Samples	T _{peak} [°C]			Residuum [%] ZrO ₂
	1 st step	2 nd step	3 th step	
ZrMOF_0eq	67.8	262.0	550.6 800.0	44.87
ZrMOF_13eq	73.9	255.2 368.8	540.7 800.0	40.20
ZrMOF_26eq	75.4	256.4 369.6	540.5 800.0	39.44
ZrMOF_52eq	79.7	258.7 385.9	550.7 800.0	37.26
ZrMOF_104eq	78.9	252.5 379.2	547.2 800.0	35.56

T_{peak}, DTG peak temperature (maximum change of weight)

Based on the fact that ideal (defect-free) (dehydroxylated) UiO-66 ZrMOF has the formula Zr₆O₆(BDC)₆, the values of weight loss (%) between 420 and 800°C (after desolvation, dehydroxylation, and modulator loss) allow us to estimate a number of 3.47, 3.17, 3.12, 3.25, 3.25 ligands in each unit of ZrMOF_0eq, ZrMOF_13eq, ZrMOF_26eq, ZrMOF_52eq and ZrMOF_104eq (Li et al. 2016). The large number of missing linker could be explained by a possible competition between the linker and DMF/modulator (with the same chemical functionality as the linker) to bind the metal node resulting in sample with missing linker or cluster defects (Han et al. 2015, Shearer et al. 2016, Winarta et al. 2020). The decrease of the percent of remaining ZrO₂ residue with increasing of modulator amount (Table1) most probably is due to a material structure change (*i.e.* missing cluster defects, the porosity changes, etc.).

N₂ adsorption-desorption isotherms

The N₂ isotherms for ZrMOF samples with or without acetic acid are presented in Figure 3. After IUPAC (Thommes et al. 2015) the recorded isotherms are type Ib and IV and the materials exhibits micropores and mesopores.

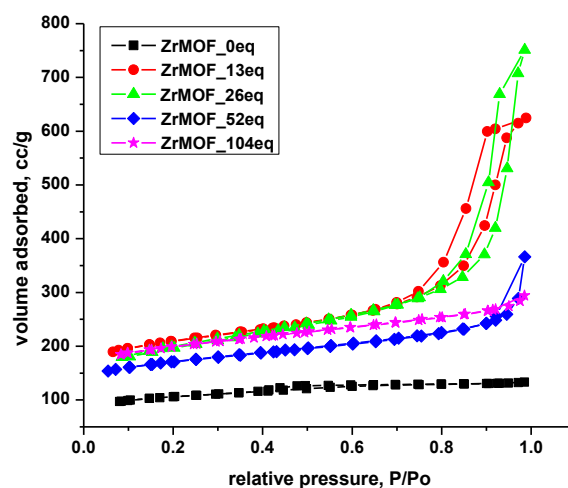


Figure 3. N₂ adsorption-desorption isotherms of ZrMOF samples

The sample ZrMOF_0eq with free AAc presents a type IVa isotherm, specific to capillary condensation, accompanied by H4 type hysteresis. The hysteresis loop H4 is specific to mesoporous materials associated with a small percent of microporosity. When acetic acid was added, the isotherms start to modify. In case of sample ZrMOF_13eq the isotherm is type IVa with H2b) hysteresis. The H2b) type of hysteresis loop is characteristic for complex pore with larger neck widths associated with pore blocking model. For these loops, the sample exhibited a plateau at the desorption branch which surpassed the plateau recorded for the adsorption branch. ZrMOF_26eq presented a type IVa isotherm with H1 hysteresis. This type of hysteresis is associated with ink-bottle pores where the width of the neck size distribution is similar to the width of the pore/cavity size distribution (Thommes et al. 2015). For samples with 52eq and 104eq of AAc, the isotherm shows the type Ib isotherm. This type of isotherm is characteristic for the materials that contain a small amount of mesopores and the majority part are micropores.

Table 2. Textural parameters

Samples	1	2	3	4	5
ZrMOF_0eq	4.57	373	261	0.20	0.11
ZrMOF_13eq	18.55	741	484	0.96	0.21
ZrMOF_26eq	28.36	703	382	1.16	0.17
ZrMOF_52eq	27.37	607	417	0.57	0.18
ZrMOF_104eq	3.77	692	486	0.46	0.22

1 - DFT, Pore diameter [nm]; 2 - BET, surface area [m²/g]; 3 - V-t method, Micropore area [m²/g]; 4 - Total pore volume [cm³/g], 5 - Alpha-S, Micropore volume [cc/g]

The specific surface area (calculated with BET method) of the materials almost doubles with the addition of the organic modulator; the highest surface area (741 m²/g) being registered for the sample with 13eq of acetic acid with a total pore volume of 0.96 cc/g (Table 2). ZrMOF_26eq shows a surface area (703 m²/g) smaller than the previous sample, but a higher total volume of pores, with a value of 1.16 cc/g. The specific surface area continues to decrease to 607 m²/g for ZrMOF_52eq with a halved value of total pore volume of 0.57 cc/g. Increasing the concentration of the modulator to 104 eq, an increase of surface area was observed (692 m²/g) with a total pore volume of 0.46 cc/g, this means that for a certain limit of the modulator concentration, the specific surface area decreases and then above this limit it starts to increase again.

Absence of modulator seems to alter the mesoporous network of the material up to a point where cavitation take place (Thommes et al. 2015). Also, acetic acid in excess (sample ZrMOF_104eq) may degrade the material and even if the porosity increases, more micropores are formed at the expense of mesopores. However, all the samples studied here have a surface area smaller than those recorded for UIO-66 samples (Wu et al. 2013).

The pore size distribution obtained with DFT method is presented in Fig. 4.

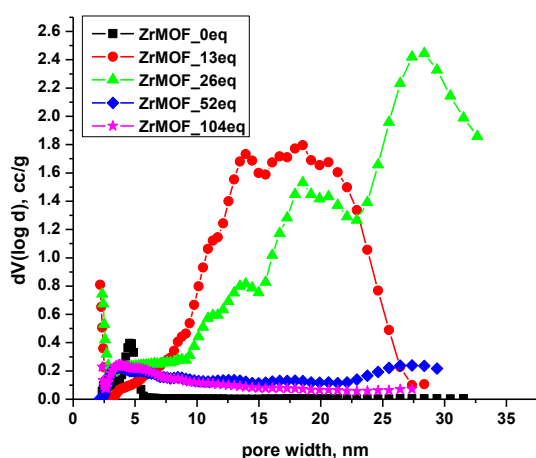


Figure 4. Pore size distribution

From Figure 4, can be observed that in case of sample with 0eq, 52eq and 104eq of AAc, the material presents a wider unimodal

distribution in the micropore and mesopore region, with pore diameter of almost 4 nm (for 0eq and 104eq) and 27 nm (for 52eq), calculated with DFT method. For sample with 13eq of AAc, the material presents a bimodal distribution with larger pores of 18 nm. We observe an increase in pore width up to sample ZrMOF_26eq becoming multimodal distribution with a diameter of pores of 28 nm.

In Figure 5 is presented the microporosity percent calculated with Alpha-S method.

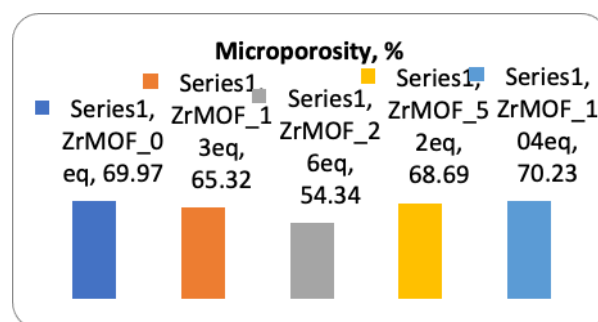


Figure 5. Microporosity percent calculated with Alpha-S method

It can be observed that the highest mesoporosity percent was obtained for sample ZrMOF_26eq. The highest content of microporosity was observed for sample without AAc and sample with the highest content of AAc with a value of ~70%.

CONCLUSIONS

In summary, we have carried out a short study of modulator effects on the surface area of some zirconium metal-organic frameworks based on terephthalic acid, in excess of Zr(IV) precursor salt. Based on thermogravimetric analysis, increasing the modulator concentration resulted in more hygroscopic materials with some missing linker defects. The presence of these defects was investigated by nitrogen adsorptions-desorption isotherms. An improvement of surface area and a change of pore structure by producing mesopores at the expense of micropores were observed in the presence of modulator. However, the amount of modulator should be carefully chosen to control the surface area, pore volume and type of porosity.

In conclusion, the insertion of a modulator during synthesis and its removal by activation process generates materials with missing linker/cluster defects even in condition of metal salt precursor excess. We showed that an increase in the concentration of modulator up to a certain value leads to an improvement of surface area and a modification of pore structure by producing mesopores at the expense of micropores.

ACKNOWLEDGEMENTS

This work was supported by the Romanian Academy, Project 4.1.

REFERENCES

- Angeli, G.K., Batzavali, D., Mavronasou, K., Tsangarakis, C., Stuerzer, T., Ott, H., Trikalitis, P.N., 2020. Remarkable Structural Diversity between Zr/Hf and Rare-Earth MOFs via Ligand Functionalization and the Discovery of Unique (4,8)-c and (4, 12)-connected Frameworks. *J. Am. Chem. Soc.* 142, 15986–15994.
<https://doi.org/10.1021/jacs.0c07081>
- Ardila-Suarez, C., Rodríguez-Pereira, J., Baldovino-Medrano, V.G., Ramírez-Caballero, G.E., 2019. An Analysis of the Effect of the Zirconium Precursor of MOF-808 on its Thermal Stability, Structural and Surface Properties. *Cryst. Eng. Comm.* 21, 1407–1415.
<https://doi.org/10.1039/C8CE01722K>
- Bai, Y., Dou, Y., Xie, L.-H., Rutledge, W., Li, J.-R. Zhou, H.-C., 2016. Zr-based metal-organic frameworks: design, synthesis, structure, and applications. *Chem. Soc. Rev.* 45, 2327.
<https://doi.org/10.1039/C5CS00837A>
- Brunauer, S., Emmett, P.H., Teller, E., 1938. Adsorption of Gases in Multimolecular Layers. *J. Am. Chem. Soc.* 60(2), 309–319.
<https://doi.org/10.1021/ja01269a023>
- Cavka, J.H., Jakobsen, S., Olsbye, U., Guillou, N., Lamberti, C., Bordiga, S., Lillerud, K.P., 2008. A new zirconium inorganic building brick forming metal organic frameworks with exceptional stability. *J. Am. Chem. Soc.* 130, 42, 13850–13851.
<https://doi.org/10.1021/ja8057953>
- Chang, Z., Li, F., Qi, X., Jiang, B., Kou, J., Sun, C., 2020. Selective and Efficient Adsorption of Au (III) in aqueous solution by Zr-based metal-organic frameworks (MOFs): An unconventionally way for gold recycling. *J. Hazard. Mater.* 391, 122175.
<https://doi.org/10.1016/j.jhazmat.2020.122175>
- Chen, Z., Hanna, S.L., Redfern, L.R., Alezi, D., Islamoglu, T., Farha, O.K., 2019. Reticular chemistry in the rational synthesis of functional zirconium cluster-based MOFs. *Coord. Chem. Rev.* 386, 32–49.
<https://doi.org/10.1016/j.ccr.2019.01.017>
- Chen, Z., Feng, L., Liu, L., Bhatt, P.M., Adil, K., Emwas, A.-H., Assen, A.H., Belmabkhout, Y., Han, Y., Eddaoudi, M., 2018. Enhanced Separation of butane Isomers via Defect Control in Fumarate/Zirconium-Based Metal Organic Framework. *Langmuir* 34, 48, 14546–14551.
<https://doi.org/10.1021/acs.langmuir.8b03085>
- Drout, R.J., Robison, L., Chen, Z., Islamoglu, T., Farha, O.K., 2019. Zirconium Metal-Organic Frameworks for Organic Pollutant Adsorption, *Trends Chem.*, 1(3), 304–3017.
<https://doi.org/10.1016/j.trechm.2019.03.010>
- Fang, X., Zong, B., Mao, S., 2018. Metal-Organic Framework-Based Sensors for Environmental Contaminant Sensing. *Nano-Micro Lett.* 10, 64.
<https://doi.org/10.1007/s40820-018-0218-0>
- Feng, D., Wang, K., Wei, Z., Chen, Y.P., Simon, C.M., Arvapally, R.K., Martin, R.L., Bosch, M., Liu, T.-F., Fordham, S., Yuan, D., Omary, M.A., Haranczyk, M., Smit, B., Zhou, H.-C., 2015. Kinetically Tuned Dimensional Augmentation as a Versatile Synthetic Route towards Robust Metal-organic Frameworks. *Nat. Commun.* 6, 6106.
<https://doi.org/10.1038/ncomms7106>
- Ghanbari, T., Abnisa, F., Wan Daud, W.M.A., 2020. A review on production of metal organic frameworks (MOF) for CO₂ Adsorption. *Sci. Total Environ.* 707, 135090.
<https://doi.org/10.1016/j.scitotenv.2019.135090>
- Guan, T., Li, X., Fang, W., Wu, D., 2020. Efficient removal of phosphate from acidified urine using UIO-66 metal-organic frameworks with varying functional groups. *Appl. Surf. Sci.* 501, 144074.

<https://doi.org/10.1016/j.apsusc.2019.144074>

Han, X., Godfrey, H.G.W., Briggs, L., Davies, A.J., Cheng, Y., Daemen, L.L., Sheveleva, A.M., Tuna, F., McInnes, E.J.L., Sun, J., Drathen, C., George, M.W., Ramirez-Cuesta, A.J., Thomas, K.M., Yang, S., Schröder M., 2018. Reversible adsorption of nitrogen dioxide within a robust porous metal-organic framework, *Nat. Nat.* 17(8), 691–696.

<https://doi.org/10.1038/s41563-018-0104-7>

Han, Y., Liu, M., Li, K., Zuo, Y., Wei, Y., Xu, S., Zhang, G., Song, C., Zhang, Z.C., Guo, X., 2015. Facile synthesis of morphology and size-controlled zirconium metal-organic framework UiO-66: the role of hydrofluoric acid in crystallization. *Cryst. Eng. Comm.* 17, 6434–6440.

<https://doi.org/10.1039/C5CE00729A>

Helal, A., Cordova K.E., Arafat, E., Usman, M., Yamani Z.H., 2020. Defect-engineering a metal-organic framework for CO₂ fixation in the synthesis of bioactive oxazolidinones. *Inorg. Chem. Front.* 7, 3571–3577.

<https://doi.org/10.1039/D0QI00496K>

Hu, Z., Peng, Y., Kang, Z., Qian, Y., Zhao, D., 2015. A Modulated Hydrothermal (MHT) Approach for the Facile Synthesis of UiO-66-Type MOFs. *Inorg. Chem.* 54(10), 4862–4868.

<https://doi.org/10.1021/acs.inorgchem.5b00435>

Jiang, K., Zhang, L., Hu, Q., Zhang X., Zhang, J., Cui, Y., Yang, Y., Li, B., 2019. Guodong Qian, A Zirconium-based Metal-organic Framework with Encapsulated Anionic Drug for Uncommonly Controlled Oral Drug Delivery. *Microporous Mesoporous Mater.* 275, 229–234.

<https://doi.org/10.1016/j.micromeso.2018.08.030>

Kalaj, M., Prosser, K.E., Cohen, S.M., 2020. Room Temperature Aqueous Synthesis of UiO-66 Derivatives via Postsynthetic Exchange, *Dalton Trans.* 49, 8841–8845.

<https://doi.org/10.1039/D0DT01939A>

Kirlikovali, K.O., Chen, Z., Islamoglu, T., Hupp, J.T., Farha, O.K., 2020. Zirconium-Based Metal-Organic Frameworks for the Catalytic Hydrolysis of Organophosphorus Nerve Agents. *ACS Appl. Mater. Interfaces* 12(16), 8130–8160.

<https://doi.org/10.1021/acsami.9b20154>

Li, B., Chrzanowski, M., Zhang, Y., Ma, S., 2016. Applications of metal-organic frameworks featuring multi-functional sites. *Coord. Chem. Rev.* 307, 106–129.

<https://doi.org/10.1016/j.ccr.2015.05.005>

Li, H.Y., Xu, J., Li, L.K., Du, X.S., Li, F.A., Xu, H., Zang, S.Q., 2017. Photochromic Properties of a Series of Zn(II)-Viologen Complexes with Structural Regulation by Anions. *Cryst. Growth Des.* 17, 6311–6319.

<https://doi.org/10.1021/acs.cgd.7b00995>

Li, B., Zhua, X., Hu, K., Li, Y., Feng, J., Shi, J., Gu, J., 2016. Defect creation in metal-organic frameworks for rapid and controllable decontamination of roxarsone from aqueous solution. *J. Hazard. Mater.* 302, 57–64.

<https://doi.org/10.1016/j.jhazmat.2015.09.040>

Liu, S., Bai, J., Huo, Y., Ning, B., Peng, Y., Li, S., Han, D., Kang, W., Gao, Z., 2020. A zirconium-porphyrin MOF-based ratiometric fluorescent biosensor for rapid and ultrasensitive detection of chloramphenicol. *Biosens. Bioelectron.* 149, 111801.

<https://doi.org/10.1016/j.bios.2019.111801>

Pan, D., Jaroniec, M., Klinik, J., 1996. Thermogravimetric evaluation of the specific surface area and total porosity of microporous carbons. *Carbon* 34(9), 1109–1113.

[https://doi.org/10.1016/0008-6223\(96\)00063-2](https://doi.org/10.1016/0008-6223(96)00063-2)

Piszczek, P., Radtke, A., Grodzicki, A., Wojtczak, A., Chojnacki, J., 2007. The new type of [Zr₆(μ₃-O)₄(μ₃-OH)₄] cluster core: Crystal structure and spectral characterization of [Zr₆O₄(OH)₄(OOCR)₁₂] (R=But, C(CH₃)₂Et). *Polyhedron* 26(3), 679–685.

<https://doi.org/10.1016/j.poly.2006.08.025>

Ravikovitch, P.I., O'Domhnaill, S.C., Neimark, A.V., Schuth, F., Unger, K.K., 1995. Capillary hysteresis in nanopores: theoretical and experimental studies of nitrogen adsorption on MCM-41, *Langmuir* 11, 4765–4772.

<https://doi.org/10.1021/la00012a030>

Ren, J., Ledwaba, M., Musyoka N.M., Langmi, H.W., Mathe, M., Liao, S., Pang W., 2017. Structural defects in metal-organic frameworks (MOFs): Formation, detection and control towards practices of interests. *Coord. Chem. Rev.* 349, 169–197.

<https://doi.org/10.1016/j.ccr.2017.08.017>

- Schaate, A., Roy, P., Godt A., Lippke, J., Waltz, F., Wiebcke, M., Behrens, P., 2011. Modulated Synthesis of Zr-Based Metal–Organic Frameworks: From Nano to Single Crystals, *Chem. Eur. J.* 17, 6643–6651.
<https://doi.org/10.1002/chem.201003211>
- Seetharaj, R., Vandana, P.V., Arya, P., Mathew, S., 2019. Dependence of solvents, pH, molar ratio and temperature in tuning metal organic framework architecture. *Arab. J. Chem.* 12, 295–315.
<https://doi.org/10.1016/j.arabjc.2016.01.003>
- Sharmin, E., Zafar, F., 2016. Introductory Chapter: Metal Organic Frameworks (MOFs), *Metal-Organic Frameworks*, Edited by Zafar, F. and Sharmin, E., IntechOpen.
<https://dx.doi.org/10.5772/64797>
- Shearer, G.C., Chavan, S., Bordiga, S., Svelle, S., Olsbye U., Lillerud K.P., 2016. Defect Engineering: Tuning the Porosity and Composition of the Metal–Organic Framework UiO-66 via Modulated Synthesis. *Chem. Mater.* 28, 3749–3761.
<https://doi.org/10.1021/acs.chemmater.6b00602>
- Silverstein, R.M., Webster, F.X., 1998. Spectrometric identification of organic compounds, Sixth Ed., John Wiley & Sons, Inc., New York, USA
- Su, J., Yuan, S., Wang, T., Lollar, C., Zuo, J., Zhang, J., Zhou, H., 2020. Zirconium Metal-organic frameworks Incorporating Tetrathiafulvalene Linkers: Robust and Redox-Active Matrices For In Situ Confinement of Metal Nanoparticles. *Chem. Sci.* 11, 1918–1925.
<https://doi.org/10.1039/C9SC06009J>
- Taddei, M., 2017. When defects turn into virtues: The curious case of zirconium-based metal-organic frameworks. *Coord. Chem. Rev.* 343, 1–24.
<https://doi.org/10.1016/j.ccr.2017.04.010>
- Thommes, M., Kaneko, K., Neimark, A.V., Olivier, J.P., Rodriguez-Reinoso, F., Rouquerol, J., Sing, K.S.W., 2015. Physisorption of gases, with special reference to the evaluation of surface area and pore size distribution (IUPAC Technical Report). *Pure Appl. Chem.* 87(9-10), 1051–1069.
<https://doi.org/10.1515/pac-2014-1117>
- Wang, S.L., Hu, F.L., Zhou, J.Y., Zhou, Y., Huang, Q., Lang, J.P., 2015. Rigidity versus Flexibility of Ligands in the Assembly of Entangled Coordination Polymers based on Bi and Tetra Carboxylates and N-Donor Ligands. *Cryst. Growth Des.* 15, 4087–4097.
<https://doi.org/10.1021/acs.cgd.5b00642>
- Wang, B., Wang, P., Xie, L.-H., Lin, R.-B., Lv, J., Li, J.-R., Che, B., 2019. A Stable Zirconium based Metal-Organic Framework for Specific Recognition of Representative Polychlorinated Dibenzo-p-dioxin Molecules. *Nat. Commun.* 10, 3861.
<https://doi.org/10.1038/s41467-019-11912-4>
- Wang, Y., Li, L., Dai, P., Yan, L., Cao, L., Gu, X., Zhao, X., 2017. Missing-node directed synthesis of hierarchical pores on a zirconium metalorganic framework with tunable porosity and enhanced surface acidity via a microdroplet flow reaction. *J. Mater. Chem. A* 5(42), 22372–22379.
<https://doi.org/10.1039/C7TA06060B>
- Winarta, J., Shan, B., Mcintyre, S.M., Ye, L., Wang, C., Liu, J., Mu, B., 2020. A Decade of UiO-66 Research: A Historic Review of Dynamic Structure, Synthesis Mechanisms, and Characterization Techniques of an Archetypal Metal–Organic Framework. *Cryst. Growth Des.* 20, 1347–1362.
<https://doi.org/10.1021/acs.cgd.9b00955>
- Xiong, Y., Fang, Y.Z., Borges, D.D., Chen, C.X., Wei, Z.W., Wang, H.P., Pan, M., Jiang, J.J., Maurin, G., Su, C.Y., 2016. Ligand and Metal Effects on the Stability and Adsorption Properties of an Isoreticular Series of Mofs Based on T-shaped Ligands and Paddle-Wheel Secondary Building Units. *Chem. Eur. J.* 22, 16147–16156.
<https://doi.org/10.1002/chem.201603299>
- Yao, S.-L., Liu, S.-J., Cao, C., Tian, X.-M., Bao, M.-N., Zheng, T.-F., 2019. Temperature- and Solvent-Dependent Structures of Three Zn(II) Metal-Organic Frameworks for Nitroaromatic Explosives Detection. *J. Solid State Chem.* 269, 195–202.
<https://doi.org/10.1016/j.jssc.2018.09.032>
- Yang, F., Li, W., Tang B., 2018. Facile synthesis of amorphous UiO-66 (Zr-MOF) for supercapacitor application. *J. Alloys Compd.* 733, 8–14.
<https://doi.org/10.1016/j.jallcom.2017.10.129>



Open Access

This article is licensed under a Creative Commons Attribution 4.0 International License, which permits use, sharing, adaptation, distribution and reproduction in any medium or format, as long as you give appropriate credit to the original author(s) and the source, provide a link to the Creative Commons license, and indicate if changes were made. The images or other third party material in this article are included in the article's Creative Commons license, unless indicated otherwise in a credit line to the material. If material is not included in the article's Creative Commons license and your intended use is not permitted by statutory regulation or exceeds the permitted use, you will need to obtain permission directly from the copyright holder.

To view a copy of this license, visit <http://creativecommons.org/licenses/by/4.0/>.

INDUCTION OF LIQUID CRYSTALLINE PROPERTIES IN Pt(II) COORDINATION COMPLEXES BASED ON TERPYRIDINE AND GALLATE LIGANDS

Evelyn POPA¹, Elisabeta I. SZERB¹, Adelina-Antonia ANDELESCU^{1*}

¹”Coriolan Drăgulescu” Institute of Chemistry, Romanian Academy, 24th Mihai Viteazu Blvd., Timișoara 300223, Romania

Corresponding author email: andelescu.ade@gmail.com

Abstract: This paper describes the induction of liquid crystalline properties into a Pt(II) complex based on the tridentate chelating N[^]N[^]N[^] ligand 2,6-di(pyridine-2-yl)pyridine-4-(1H)-one, following a strategy reported previously by our group, respectively using a lipophilic gallate unit. Two structurally different Pt(II) species containing one or two gallate units were obtained in the same reaction and were characterized by spectroscopic (FT-IR and ¹H NMR) and analytic (elemental analysis) methods. Their liquid crystalline behaviour was assessed by polarized optical microscopy (POM) observations.

Keywords: Pt(II) metallomesogens, terpyridine Pt(II) coordination complexes, polarized optical microscopy.

INTRODUCTION

Metallomesogens (metal containing liquid crystals) based on *d*-block metal centres are appealing for widespread high-tech, due to the properties arising from both classes: i) metal centres: optical, electronic, magnetic, conductive, dichroic, etc. (Ma *et al.* 2012, Kettle 1996, Darkwah *et al.* 2020, Sanda 2014, Pessoa *et al.* 2009) and ii) liquid crystals: anisotropy of the physical properties, fluidity, stimuli responsiveness, supramolecular complex dynamic and adaptive ordering, etc. (Donnio 2014, Pucci and Donnio 2014). Moreover, their final properties may be improved due to cumulative and/or synergistic effects. Owing to their enhanced properties, metallomesogens are currently under studies for applications in electroluminescent displays (Wu *et al.* 2018a, Rajendiran *et al.* 2020), or as active materials for the fabrication of sensors (Cuerva *et al.* 2016, Cuerva *et al.* 2020, Motoc *et al.* 2019), etc.

A particular interest has been granted to Pt(II) due to the thermodynamic preference of the metal ions to form square planar complexes with strong-field ligands (Williams 2007), property that favours key features regarding absorption, luminescence and other excited state properties. Moreover, it makes it favourite for inducing liquid crystalline properties with respect to other bulkier geometry metals like octahedral Ir(III), Ru(II), tetrahedral Cu(I), Zn(II) etc. (Wu *et al.* 2018b). Therefore, Pt(II) metallomesogens are intensively researched in

optoelectronics (Sato *et al.* 2012, Yang *et al.* 2018, Qian *et al.* 2020). Terpyridines (*tpy*) are commonly being employed as ligands, due to their ability to coordinate a wide variety of metal centres and also because their derivatives show great potential in inducing structural variations, thus obtaining five-, six and nine-coordinate geometries (Kumar *et al.* 2016).

Previously we showed in the case of a Pt(II) complex containing a *tpy* ligand substituted in the apical position with a long alkyl chain (**L-tpyOR**), that a moderately coordinating gallate unit (**Gal**) can function both as a monodentate ligand, in fulfilling the coordination sphere of Pt(II) or as counterion (Andelescu *et al.* 2020). Furthermore, this strategy allowed us to easily induce liquid crystallinity in the final complex Pt(II) complexes.

Herein we report that by using 2,6-di(pyridine-2-yl)pyridine-4-(1H)-one (**L-tpyOH**), the obtainment of two Pt(II) species containing one or two gallate units from a single reaction was achieved (Figure 1).

The two Pt(II) species containing one or two gallate units were characterized by FT-IR and NMR spectroscopies and elemental analysis. Moreover, in case of **Pt_1** and **Pt_2** complexes the liquid crystalline behaviour was assessed by polarized optical microscopy (POM) observations.

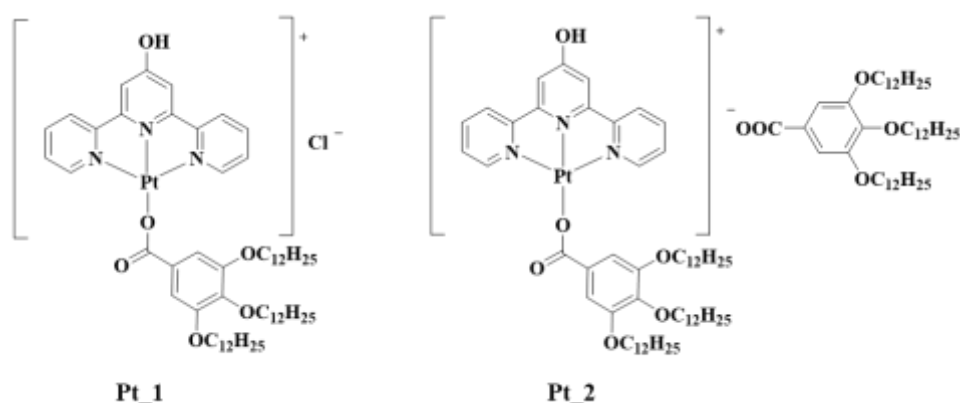


Figure 1. The proposed structures of the Pt(II) complexes **Pt_1** and **Pt_2**.

MATERIALS AND METHODS

All commercially available starting materials were used as received without further purification. The ligand **L_tpyOH**, $\text{PtCl}_2((\text{CH}_3)_2\text{SO})_2$ and the silver complex of 3,4,5-tridodecyloxybenzoic acid (**Ag(Gal)**) were obtained according to reported procedures (Schubert *et al.* 2002, Kukushkin *et al.* 2002, Szerb *et al.* 2013). Infrared spectra (KBr) in the range $4000\text{--}400\text{ cm}^{-1}$ were recorded on a Cary 630 FT-IR spectrophotometer. ^1H NMR experiments were recorded on a Bruker Fourier 300 MHz spectrometer in DMSO- d_6 or CDCl_3 using tetramethylsilane (TMS) as internal standard. Elemental analysis C, H and N was performed on a Flash 2000 analyser, by ThermoFisher Scientific, using 1 mg of sample. Two determinations were performed and the average value was used. The optical textures of mesophases were carried out using an Olympus BX53M polarizing microscope (POM) equipped with Linkam hot-stage. Images of the various phases were recorded using an Olympus UC90 camera.

EXPERIMENTAL SECTION

Synthesis of the $[\text{L_tpyOH}(\text{PtCl})]^+\text{Cl}^-$ precursor
 $[\text{L_tpyOH}(\text{PtCl})]^+\text{Cl}^-$ was synthesized by a slight modification of a method reported in literature for similar derivatives (Annibale *et al.* 1995): a solution of **L_tpyOH** (0.450 g, 1.749 mmol) in 20 mL CH_2Cl_2 was added dropwise over a suspension of $\text{PtCl}_2((\text{CH}_3)_2\text{SO})_2$ (0.739 g, 1.749 mmol) in 130 mL CH_2Cl_2 . The reaction mixture was stirred at room temperature for 4 hours, filtered and washed diethyl ether, yielding a yellow precipitate

$[\text{L_tpyOH}(\text{PtCl})]^+\text{Cl}^-$: yellow precipitate (0.756g, 1.467 mmol, 84%).

FT-IR (KBr, cm^{-1}): 3317 (br, H_2O), 1607-1455(ν (C=C) and ν (C=N)), 442 (ν (Pt-N)).

$^1\text{H-NMR}$ (300 MHz, DMSO- d_6 , δ -ppm): 8.90 (d, $J = 5.2$ Hz, 2H), 8.43 (d, $J = 5.8$ Hz, 6H), 7.86 (s, 2H), 7.65 (s, 2H).

Synthesis of Pt_1 and Pt_2

A solution of **Ag(Gal)** (0.456 g, 0.582 mmol) in 20 mL CHCl_3 was added dropwise over a suspension of $[\text{L_tpyOH}(\text{PtCl})]^+\text{Cl}^-$ (0.15 g, 0.291 mmol) in 20 mL CHCl_3 . The reaction mixture was stirred at room temperature for 2 hours, filtered and washed with CHCl_3 . The mother liquor was taken to dryness. The residue was triturated with hexanes, separated by centrifugation yielding a yellow precipitate (**Pt_2**). The supernatant was evaporated under reduced pressure to give **Pt_1**.

Pt_1: yellow precipitate (0.275 g, 0.195 mmol, 67%)

FT-IR (KBr, cm^{-1}): 2955, 2922, 2852 (C-H stretch), 1635 ($\nu_{\text{as}}(\text{COO}^-)$), 1585-1425 (ν (C=C) and ν (C=N)), 1338 ($\nu_{\text{s,coordinated}}(\text{COO}^-)$), 445 (ν (Pt-N)).

^1H NMR (300 MHz, CDCl_3 , δ -ppm): 8.49 (d, $J = 5.72$ Hz, 1.52 Hz, 2H), 8.09 (td, $J = 7.89$ Hz, 7.87 Hz, 1.56 Hz, 2H), 7.83 (d, $J = 8.02$ Hz, 2H), 7.42 (overlapped peaks, 4H), 7.35 (s, 2H) 4.05 (overlapped peaks, 6H), 3.69 (broad s, 1H, OH), 2.01 – 1.65 (m, 6H), 1.62-1.14 (overlapped peaks, 54 H), 0.97- 0.73 (m, 9H).

Anal. Calcd. for $\text{C}_{59}\text{H}_{91}\text{ClN}_3\text{O}_6\text{Pt}\cdot\text{H}_2\text{O}$ (MW = : C, 59.7; H, 7.95; N, 3.54; Found: C, 59.83; H, 7.68; N, 3.31.

Pt_2: orange precipitate (0.02 g, 0.0109 mmol, 3.75 %)

IR (KBr, cm^{-1}): 2953, 2920, 2851 (C-H stretch), 1635 ($\nu_{\text{as}}(\text{COO}^-)$), 1585-1425 ($\nu(\text{C}=\text{C})$ and $\nu(\text{C}=\text{N})$), 1555 ($\nu_{\text{s,ionic}}(\text{COO}^-)$), 1342 ($\nu_{\text{s,coordinated}}(\text{COO}^-)$), 445 ($\nu(\text{Pt}-\text{N})$).

$^1\text{H NMR}$ (300 MHz, CDCl_3 , δ -ppm): 8.48 (dd, $J = 5.7, 1.5$ Hz, 2H), 8.09 (td, $J = 7.9, 1.6$ Hz, 2H),

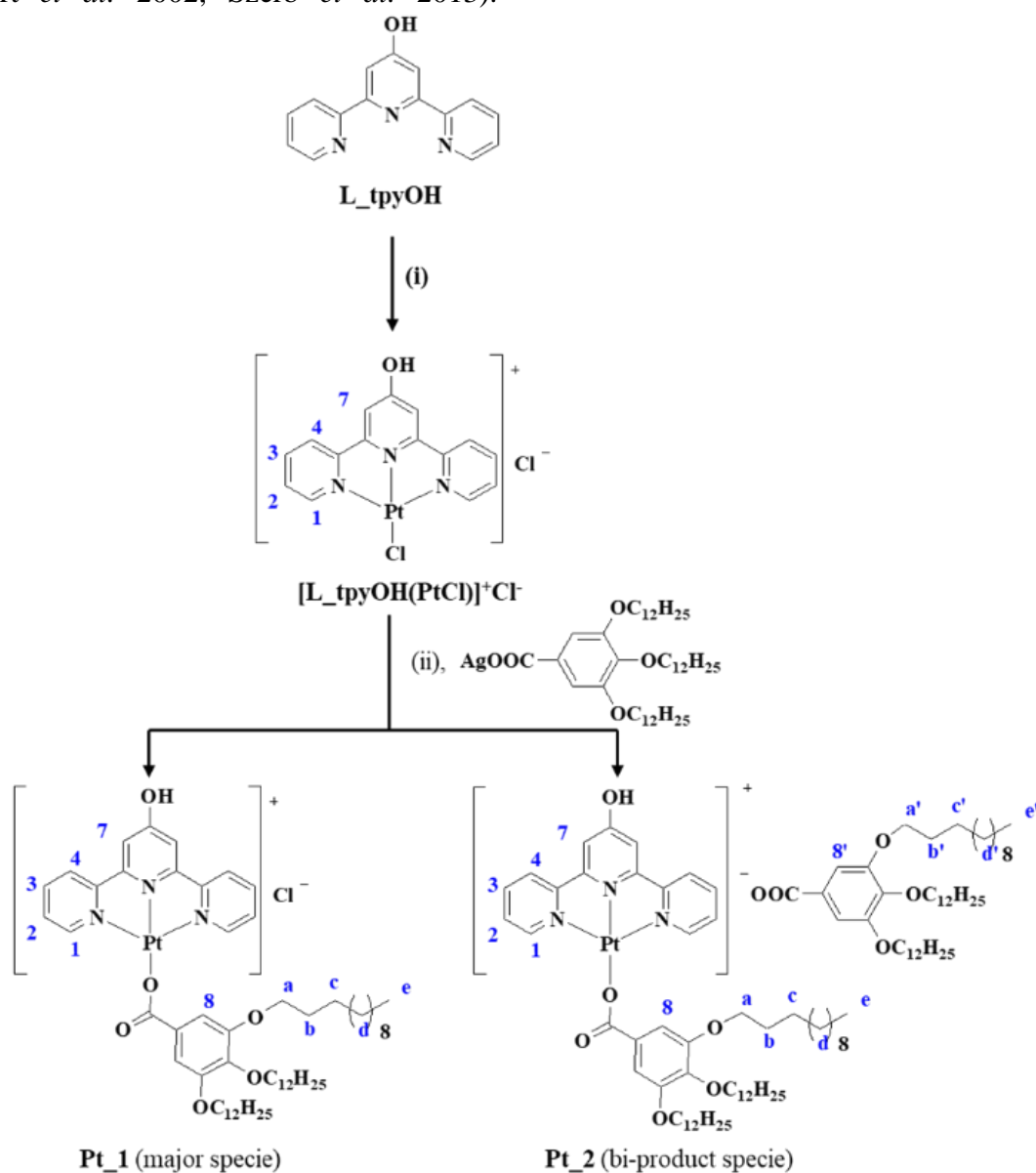
7.78 (d, $J = 7.9$ Hz, 2H), 7.53 – 7.34 (overlapped peaks, 4H), 7.32 (s, 2H), 7.05 (s, 2H), 4.06 (dt, $J = 10.5, 6.4$ Hz, 12H), 2.88 (broad s, 1H, OH), 1.96 – 1.68 (m, 12H), 1.57 – 1.18 (m, 108H), 0.91 – 0.80 (m, 18H).

Anal. Calcd. for $\text{C}_{101}\text{H}_{165}\text{N}_3\text{O}_{11}\text{Pt}$ (MW = 1791.21 g/mol): C, 67.68; H, 9.28; N, 2.34; Found: C, 67.99; H, 9.68; N, 2.31.

RESULTS AND DISCUSSIONS

The synthesis of **L_tpyOH** and the silver complex of 3,4,5-tridodecyloxybenzoic acid were carried out as previously reported (Schubert *et al.* 2002, Szerb *et al.* 2013).

Complex $[\text{L_tpyOH}(\text{PtCl})]^+\text{Cl}^-$ was used as precursor to obtain **Pt_1** and **Pt_2** complexes, by reacting it with 2 equivalents of **Ag(Gal)** (Scheme 1).



Scheme 1. Reaction pathway of complexes **Pt_1** and **Pt_2** with **L_tpyOH** (atom labelling in blue). Reagents and conditions: (i) $\text{PtCl}_2((\text{CH}_3)_2\text{SO})_2$, MeOH, r.t., 2 h; (ii) Ag(Gal), CHCl_3 , r.t., 2 h.

Differently from the previously employed Pt(II) complex containing the ligand **L_tpyOR** that when reacted with the silver salt of the gallate

Ag(Gal) (Andelescu *et al.* 2020) yielded exclusively the complex containing two gallates, herein two species were obtained, probably due to the strong activating group in the apical position. **Pt_1** was obtained as major product and complex **Pt_2** as side product (Scheme 1). All attempts to obtain **Pt_2** as major product complex by changing the reaction conditions (temperature, solvent or reaction time) or reactants ratio failed. Due to the higher solubility of **Pt_2** in hexane, we were able to separate and characterize the compounds. Also, we have investigated the mesomorphic behaviour by POM.

FT-IR spectroscopy.

By comparing the spectra of the free ligand (**L_tpyOH**) with that of **[L_tpyOH(PtCl)]⁺Cl⁻**, Figure 2, the shifts of the characteristic absorption bands corresponding to $\nu_{C=C}$ and $\nu_{C=N}$ confirm the successful coordination of Pt(II) centre via the nitrogen atoms of the ligand (Burger *et al.* 2001). Also, in the spectra of the complex, the characteristic absorption band corresponding to $\nu(Pt-N)$ is observed at 442 cm^{-1} (Allen and Theophanides 1964).

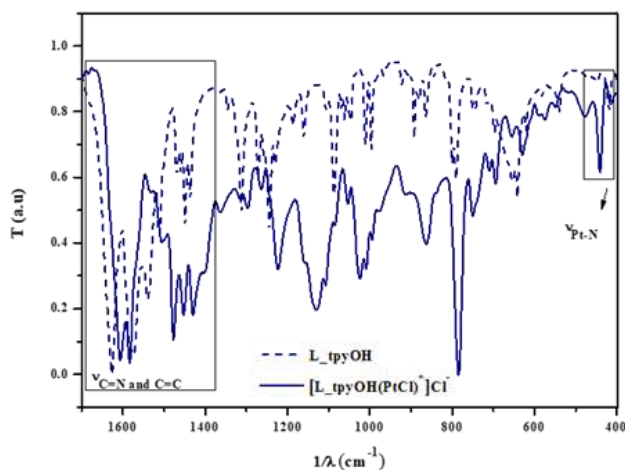


Figure 2. FT-IR spectra of **[L_tpyOH(PtCl)]⁺Cl⁻** plotted against **L_tpyOH** free ligand.

Moreover, after the exchange of the chlorine ligand and/or counterion with the gallate unit, the dual coordination mode of the gallate group can be noticed by comparing the spectra of the **Pt_1** and **Pt_2** complexes (Figure 3). In particular, the FT-IR spectra of complex **Pt_1** presents the characteristic absorption

bands specific of COO^- stretching frequencies: the ν_{as} at 1635 cm^{-1} , and ν_s at 1340 cm^{-1} ($\Delta = 295$ cm^{-1}). Based on literature data (Deacon and Phillips 1980), this value corresponds to a carboxylate unit, which is coordinated to the metal centre. In case of **Pt_2**, two different symmetric COO^- stretching frequencies are observed at: 1555 cm^{-1} (ionic carboxylate) and 1340 (coordinated carboxylate), thus giving a separation (Δ) of 80 and respectively 295 cm^{-1} as seen from Figure 3. The first value corresponds to an ionic carboxylate unit, while the later to a coordinated one.

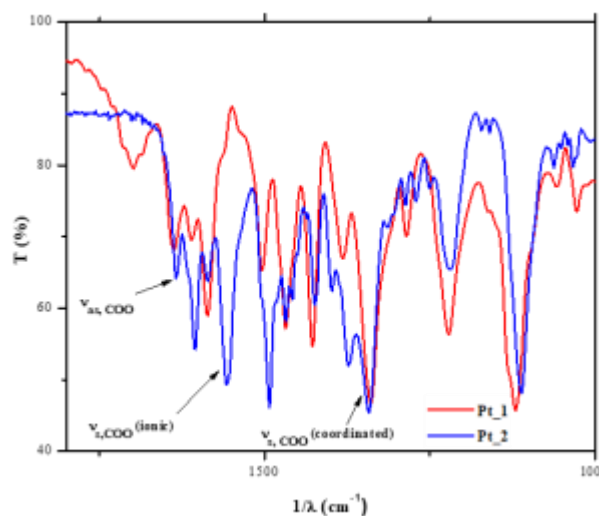


Figure 3. FT-IR spectra of **Pt_1** and **Pt_2**.

¹H-NMR spectroscopy

In the ¹H-NMR spectra, significant shifts of the aromatic signals associated with the *tpy* protons were observed after complexation. The dual coordination mode of gallate unit is demonstrated also by the ¹H-NMR spectroscopy, respectively the aromatic protons belonging to the gallate (Gal) groups have different chemical shifts when coordinated to the metal centre as monodentate ligand (H^8) or when they ensure the neutrality of the complex as negatively charged anion (H^{8-}), as shown in Figure 4. In the case of **Pt_1** and **Pt_2**, the aromatic protons belonging to the gallate (Gal) groups have different chemical shifts (Figure 4). In particular, the aromatic proton (H^8) of the gallate unit is observed at 7.35 ppm for complex **Pt_1** and at 7.32 ppm for complex **Pt_2**, showing a coordinated mode, whereas for **Pt_2** the aromatic protons H^{8-} , corresponding to the gallate counterion appear at 7.05 ppm.

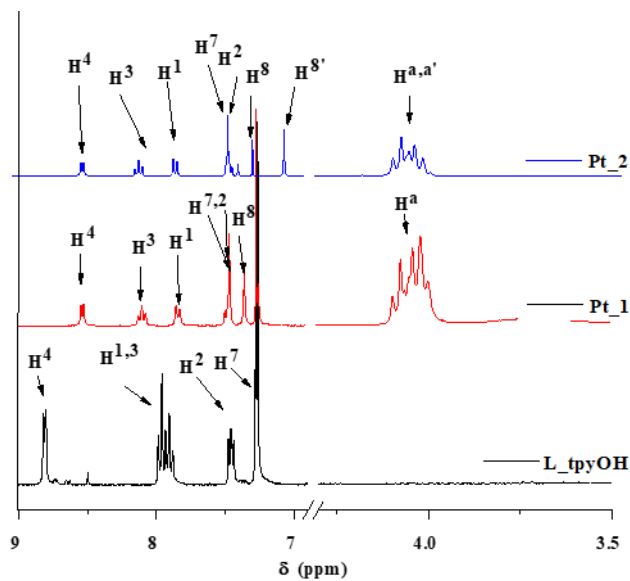


Figure 4. $^1\text{H-NMR}$ spectra of ligand L_tpyOH , Pt_1 and Pt_2 recorded in CDCl_3 .

Mesomorphic properties

The mesomorphic properties of both Pt_1 and Pt_2 complexes was assessed by POM observations. Pt_1 decomposes before the transition into the isotropic phase, while Pt_2 has a clearing point at 213°C .

The investigation of the monosubstituted specie Pt_1 by POM microscopy revealed mesomorphic behaviour on heating. A transition around 83°C from a solid state to a liquid crystalline state is observed, the texture pointing towards a lamellar phase (Figure 5a). The compound decompose before melting around 250°C . Regarding complex Pt_2 , it exhibit between 70°C and 213°C a columnar phase as identified by the focal-conic texture with homeotropic zones developed on cooling (Figure 5b).

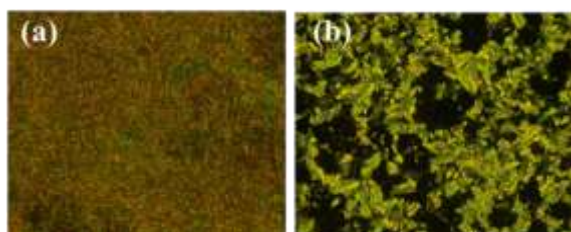


Figure 5. POM micrographs obtained for complex a) Pt_1 on heating at 200°C and b) Pt_2 at 175°C on cooling from the isotropic liquid.

CONCLUSIONS

The synthesis of two Pt(II) species, Pt_1 and Pt_2 , containing one or two gallate units from a single reaction was achieved using 2,6-di(pyridine-2-yl)pyridine-4-(1*H*)-one as tridentate ligand. The final complexes were characterized through FT-IR and $^1\text{H-NMR}$ and elemental analysis.

FT-IR spectroscopy provided information regarding the dual coordination mode of the gallate unit. In case of Pt_1 the large separation value of the characteristic absorption bands of the carboxylate unit (asymmetrical and symmetrical, $\Delta = 295 \text{ cm}^{-1}$) suggest that the gallate unit is coordinated to the Pt(II) metal centre, having chlorine as counterion, whereas in case of Pt_2 two different symmetric COO^- stretching frequencies were observed, indicating that in this case both the displacement of the chlorine counterion and ligand took place.

Furthermore, the chemical shifts of complex Pt_1 of the aromatic and aliphatic protons were assigned based on $^1\text{H NMR}$ acquisitions.

The mesomorphic properties of both Pt_1 and Pt_2 complexes were investigated by POM. Pt_1 developed a texture pointing towards a lamellar phase, while Pt_2 showed a typical columnar texture.

ACKNOWLEDGEMENTS

Authors acknowledge the Romanian Academy, Program 4. A.A.A. is grateful for an “Ion Heliade Radulescu” mobility scholarship.

REFERENCES

- Allen, A.D., Theophanides, T., 1964. Platinum(II) Complexes: Infrared Spectra in the $300\text{--}800 \text{ cm}^{-1}$ Region. *Can. J. Chem.* 42(7), 1551–1554.
<https://doi.org/10.1139/v64-238>
- Andelescu, A.-A., Heinrich, B., Spirache, M.A., Voirin, E., La Deda, M., Di Maio, G., Szerb, E.I., Donnio, B., Costisor, O., 2020. Playing with Pt^{II} and Zn^{II} Coordination to Obtain Luminescent Metallomesogens. *Chem. Eur. J.* 26, 4850–4860.
<https://doi.org/10.1002/chem.202000124>
- Annibale, G., Brandolisio, M., Pitteri, B., 1995. New routes for the for the synthesis of chloro(diethylenetriamine) platinum(II) chloride and chloro(2,2' : 6',2''-terpyridine)

platinum(II) chloride dihydrate. *Polyhedron* 14(3), 451–453.

[https://doi.org/10.1016/0277-5387\(94\)00408-7](https://doi.org/10.1016/0277-5387(94)00408-7)

Burger, K., Wagner, F.E., Vértés, A., Bencze, É., Mink, J., Labádi, I., Nemes-Vetéssy, Z., 2001. Structural Study of Terpyridine and O-Phenanthroline Complexes of Iridium(III). *J. Phys. Chem. Solids* 62(11), 2059–2068.

[https://doi.org/10.1016/S0022-3697\(01\)00075-0](https://doi.org/10.1016/S0022-3697(01)00075-0)

Cuerva, C., Campo, J.A., Cano, M., Lodeiro, C., 2016. Platinum(II) Metallomesogens: New External-Stimuli-Responsive Photoluminescence Materials. *Chem. Eur. J.* 22(29), 10168–10178.

<https://doi.org/10.1002/chem.201601115>

Cuerva, C., Campo, J.A., Cano, M., Caño-García, M., Otón, J.M., Lodeiro, C. 2020. Aggregation-induced emission enhancement (AIEE)-active Pt(II) metallomesogens as dyes sensitive to Hg²⁺ and dopant agents to develop stimuli-responsive luminescent polymer materials. *Dyes Pigm.* 175, 108098.

<https://doi.org/10.1016/j.dyepig.2019.108098>

Darkwah, W.K., Sandrine, M.K.C., Adormaa, B.B., Teye, G.K., Puplampu, J.B., 2020. Solar Light Harvest: Modified d-Block Metals. *Photocatalysis. Catal. Sci. Technol.* 10(16), 5321–5344.

<https://doi.org/10.1039/C9CY02435B>

Deacon, G., Phillips R. J., 1980. Relationships between the Carbon-Oxygen Stretching Frequencies of Carboxylato Complexes and the Type of Carboxylate Coordination. *Coord. Chem. Rev.* 33(3), 227–250.

[https://doi.org/10.1016/S0010-8545\(00\)80455-5](https://doi.org/10.1016/S0010-8545(00)80455-5)

Donnio, B., 2014. Liquid-crystalline metallodendrimers. *Inorg. Chim. Acta* 409, 53–67.

<https://doi.org/10.1016/j.ica.2013.07.045>

Kettle, S.F.A. *Magnetic Properties of Transition Metal Complexes* 1996. In *Physical Inorganic Chemistry: A Coordination Chemistry Approach*, Springer Berlin Heidelberg: Berlin, Heidelberg.

https://doi.org/10.1007/978-3-662-25191-1_9

Kukushkin, V.Y., Pombeiro A.J.L., Ferreira C.M.P., Elding L.I., 2002. In *Inorganic Syntheses: Dimethylsulfoxide Complexes of*

Platinum(II): K[PtCl₃(Me₂SO)], cis-[PtCl₂L(Me₂SO)] (L=Me₂SO, MeCN), [PtCl(μ-Cl)(Me₂SO)]₂, and [Pt(Me₂SO)₄](CF₃SO₃)₂. John Wiley & Sons, Inc.

Kumar, N.S.S., Shafikov, M.Z., Whitwood, A.C., Donnio, B., Karadakov, P.B., Kozhevnikov, V.N., Bruce, D.W., 2016. Mesomorphism and Photophysics of Some Metallomesogens Based on Hexasubstituted 2,2':6', 2''-Terpyridines. *Chem. Eur. J.* 22(24), 8215–8233.

<https://doi.org/10.1002/chem.201505072>

Ma, D.-L., Ma, V. P.-Y., Chan, D. S.-H., Leung, K.-H., He, H.-Z., Leung, C.-H., 2012. Recent advances in luminescent heavy metal complexes for sensing. *Coord. Chem. Rev.* 256(23–24), 3087–3113.

<https://doi.org/10.1016/j.ccr.2012.07.005>

Motoc, S., Cretu, C., Costisor, O., Baciú, A., Manea, F., Szerb, E.I., 2019. Cu(I) Coordination Complex Precursor for Randomized CuOx Microarray Loaded on Carbon Nanofiber with Excellent Electrocatalytic Performance for Electrochemical Glucose Detection. *Sensors* 19(24), 5353.

<https://doi.org/10.3390/s19245353>

Pessoa, J., Correia, I., Gonçalves, G., Tomaz, A. I., 2009. Circular Dichroism in Coordination Compounds. *J. Arg. Chem. Soc.* 97(1), 151–165.

<https://doi.org/10.1021/ic50018a026>

Pucci, D., Donnio, B., 2014. Metal-Containing Liquid Crystals. In *Handbook of Liquid Crystals*. 2nd ed., Vol. 5: Non-Conventional Liquid Crystals, Weinheim: Wiley-VCH, pp. 175–241.

<https://doi.org/10.1002/9783527671403.hlc077>

Qian, G., Yang, X., Wang, X., Herod, J.D., Bruce, D.W., Wang, S., Zhu, W., Duan, P., Wang, Y., 2020. Chiral Platinum-Based Metallomesogens with Highly Efficient Circularly Polarized Electroluminescence in Solution-Processed Organic Light-Emitting Diodes. *Adv. Opt. Mater.* 8(20), 2000775.

<https://doi.org/10.1002/adom.202000775>

Rajendiran, K., Yoganandham, S.T., Arumugam, S., Arumugam, D., Thananjeyan, K., 2020. An Overview of Liquid Crystalline Mesophase Transition and Photophysical Properties of “f Block,” “d Block,” and (SCO)

Spin-Crossover Metallomesogens in the Optoelectronics. *J. Mol. Liq.* 2020, 114793.

<https://doi.org/10.1016/j.molliq.2020.114793>

Sanda, F., 2015. Transition Metal Containing Polymers. In *Encyclopedia of Polymeric Nanomaterials*, Springer Berlin Heidelberg: Berlin, Heidelberg, pp. 1–6.

https://doi.org/10.1007/978-3-642-36199-9_383-1

Sato, T., Awano, H., Haba, O., Katagiri, H., Pu, Y.-J., Takahashi, T., Yonetake, K., 2012. Synthesis, Characterization, and Polarized Luminescence Properties of Platinum(II) Complexes Having a Rod-like Ligand. *Dalton Trans.* 41(27), 8379–8389.

<https://doi.org/10.1039/C2DT30071K>

Schubert, U.S., Schmatloch, S., Precup, A., 2002. Access to supramolecular polymers: Large scale synthesis of 4'-chloro-2,2':6',2''-terpyridine and an application to poly(propylene oxide) telechelics. *Des. Monomers Polym.* 5, 211–221.

<https://doi.org/10.1163/156855502760157935>

Szerb, E.I., Pucci, D., Crispini, A., La Deda, M., 2013. Soft Luminescent Materials Based on Ag(I) Coordination Complexes. *Mol. Cryst. Liq. Cryst.* 573, 34–45.

<https://doi.org/10.1080/15421406.2013.763335>

Williams, J.A.G., 2007. Photochemistry and Photophysics of Coordination Compounds: Platinum. *Top. Curr. Chem.* 281, 205–268.

https://doi.org/10.1007/128_2007_134

Wu, X., Xie, G., Cabry, C.P., Xu, X., Cowling, S.J., Bruce, D.W., Zhu, W., Baranoff, E., Wang, Y., 2018a. Linearly Polarized Electroluminescence from Ionic Iridium Complex-Based Metallomesogens: The Effect of Aliphatic-Chain on Their Photophysical Properties. *J. Mater. Chem. C* 6, 3298–3309.

<https://doi.org/10.1039/C7TC05421A>

Wu, X., Zhu, M., Bruce, D.W., Zhu, W., Wang, Y., 2018b. An overview of phosphorescent metallomesogens based on platinum and iridium. *J. Mater. Chem. C* 6, 9848–9860.

<https://doi.org/10.1039/C8TC02996B>

Yang, X., Wu, X., Zhou, D., Yu, J., Xie, G., Bruce, D.W., Wang, Y., 2018. Platinum-Based Metallomesogens Bearing a Pt(4,6-Dfppy)(Acac) Skeleton: Synthesis, Photophysical Properties and Polarised Phosphorescence Application. *Dalton Trans.* 47(38), 13368–13377.

<https://doi.org/10.1039/C8DT03017K>



Open Access

This article is licensed under a Creative Commons Attribution 4.0 International License, which permits use, sharing, adaptation, distribution and reproduction in any medium or format, as long as you give appropriate credit to the original author(s) and the source, provide a link to the Creative Commons license, and indicate if changes were made. The images or other third party material in this article are included in the article's Creative Commons license, unless indicated otherwise in a credit line to the material. If material is not included in the article's Creative Commons license and your intended use is not permitted by statutory regulation or exceeds the permitted use, you will need to obtain permission directly from the copyright holder.

To view a copy of this license, visit <http://creativecommons.org/licenses/by/4.0/>.

SCIENTIFIC EVENT: STUDENT SCIENTIFIC SESSION AT FACULTY OF FOOD ENGINEERING, TOURISM AND ENVIRONMENTAL PROTECTION, 2020

Dana Maria COPOLOVICI

“Aurel Vlaicu” University of Arad, Faculty of Food Engineering, Tourism and Environmental Protection; Romania, 2 Elena Dragoi St., Arad, 310330, Romania

**Corresponding author: dana.copolovici@uav.ro*

Abstract: Faculty of Food Engineering, Tourism and Environmental Protection from “Aurel Vlaicu” University of Arad organized on November 26rd -27th 2020 The 18th Edition of the Student Scientific Session. Within the general program, 10 parallel sessions were carried out. In the present article, we have been focused on the first on-line edition, due to SARS-CoV-2 pandemic, with 2 sessions that were organized by the Faculty of Food Engineering, Tourism and Environmental Protection: (1) Engineering and Environmental Science, Environmental Protection, Biodiversity, Health, Applied Biology, and (2) Food Technology, Food Engineering, Nutrition, Food Quality and Food Security, Agrotourism Management, Sustainability. In those three sessions were held 15 oral scientific presentations and 13 posters by students from diverse Romanian universities. This event attracted more than 70 attendees from academia.

Keywords: scientific students’ symposium, scientific presentations, posters, interdisciplinary, science and engineering, ethics.

Faculty of Food Engineering, Tourism and Environmental Protection from “Aurel Vlaicu” University of Arad, Romania, organized on November 26rd -27th 2020 The 18th Edition of the Student Scientific Session at Faculty of Food Engineering, Tourism and Environmental Protection. Since 2016, this event was organized each year, in Arad, Romania and due to its heterogeneity in scientific topics many students presented their scientific results (>200 presentations) and attendees from academia were present.

The program contains 2 sessions:

- Session I: Environmental Science and Engineering, Environmental Protection, Biodiversity, Health, Applied Biology;
- Session II: Food Technology, Food Engineering, Nutrition, Food Quality and Food Security, Agrotourism Management, Sustainability.

Due to SARS-CoV-2 pandemic, the event held in 2020 was on-line, via ZOOM, and the diverse results obtained in University of Agricultural Sciences and Veterinary Medicine, Cluj-Napoca; Banat University of Agricultural Sciences and Veterinary Medicine „King Michael 1st of Romania” from Timisoara; ”Dunărea de Jos” University from Galati; Politehnica University from Bucharest; University of Agronomic Sciences

and Veterinary Medicine from Bucharest; “Alexandru Ioan Cuza” University from Iasi; University of Oradea; „Babeş-Bolyai” University from Cluj-Napoca, and „Aurel Vlaicu” of Arad were presented.

The virtual scientific meetings, including symposiums, conferences were held and continue to be held in hybrid or on-line in 2020 due to COVID-19 pandemic (Hoogendoorn and Aye, 2020, Kindstedt, 2019, Olena, 2020, Woolston, 2020).

The main objectives of this free of charge symposium are:

- To connect students and research groups, share knowledge, establish research partnerships;
- To present and promote the scientific, engineering, and technological development research results obtained by students from bachelor, master, and doctoral (Ph.D.) studies and their research groups from national research institutes and universities;
- To stimulate invention, innovation and raising awareness of the importance of networking, socializing, brain-storming, debate;
- To enhance the importance and role in life and society of scientific research, hear talks and posters’ presentations, raise

questions, open new research perspectives, to participate to the award ceremony.

The first day of the symposium begun with a Welcome Speech in which the Rector of “Aurel Vlaicu” University, Prof. Dr. Ramona Lile; Vice Rector Prof. Dr. Codruta Stoica, Vice Rector Prof. Dr. Alexandru Popa, Dean of Faculty of Food Engineering, Tourism and Environmental Protection: Assoc. Prof. Dr. Eng. Virgiliu Ciutina; Director of Department of Technical and Natural Sciences: Assoc. Prof. Dr. Eng. Monica Lungu, and Research responsible of Department of Technical and Natural Sciences: Prof. Dr. Habil. Dana Copolovici had presented the event, and welcomed all the participants (Fig. 1).

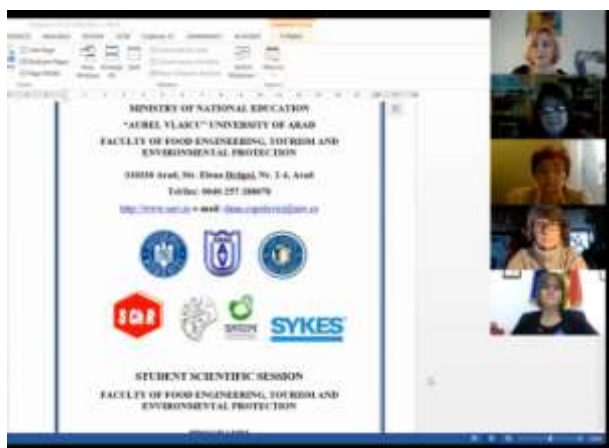


Fig. 1. Welcome speech from the Rector of “Aurel Vlaicu” University, Prof. Dr. Ramona Lile; Vice Rector Prof. Dr. Codruta Stoica, Vice Rector Prof. Dr. Alexandru Popa, Dean of Faculty of Food Engineering, Tourism and Environmental Protection: Assoc. Prof. Dr. Eng. Virgiliu Ciutina; Director of Department of Technical and Natural Sciences: Assoc. Prof. Dr. Eng. Monica Lungu, and Research responsible of Department of Technical and Natural Sciences: Prof. Dr. Habil. Dana Copolovici.

In the first session were presented nine oral presentations and six posters with wide exciting themes: anthropogenic and biogenic pollutants’ evaluation and monitoring in soil, water, wastewater, and air; applications of essential oils, agricultural waste management, health related topics: influence of food additives and COVID-19 on human immune system, relationship between Alzheimer's disease and diabetes, etc.

- Oral presentations:

1st Prize: Gherghe Radu-Ștefan
Politehnica University from Bucharest, Romania

2nd Prize: Flavia Borteș
“Aurel Vlaicu” University, Romania

3rd Prize: Chereji Bianca Denisa
“Aurel Vlaicu” University, Romania

Honorary Mention:

Ionela Șuibea
“Aurel Vlaicu” University of Arad, Romania

Mirabela-Elena Raț
“Aurel Vlaicu” University of Arad, Romania

-Poster presentations:

1st Prize: Angela Corina Popițanu
University of Oradea, Romania

2nd Prize: Monica Tășchină
“Aurel Vlaicu” University, Romania

3rd Prize: Adrian Bodescu
“Babes-Bolyai” University, Cluj-Napoca, Romania.

The judges of this session which evaluated all the presentations were: Prof. dr. habil. Florentina Munteanu, Prof. dr. habil. Lucian Copolovici, Assoc Prof. dr. habil. Dorina Chambre, and Assoc Prof. dr. Virgiliu Ciutina from “Aurel Vlaicu” University.

In the second session, held on the second day of the event, were presented six oral presentations and nine posters with interesting themes: obtaining and evaluation of innovative and sustainable food products, ethical and security aspects of food products, evaluation of potential uses of plants extracts.

- Oral presentations:

1st Prize: Anamaria Mihaly
University of Agricultural Sciences and Veterinary Medicine, Cluj-Napoca; Romania.
2nd Prize: Maria Florina Roșca

University of Agricultural Sciences and Veterinary Medicine, Cluj-Napoca; Romania.

3rd Prize: Ioana Isabela Dumitraşcu

University of Agricultural Sciences and Veterinary Medicine, Cluj-Napoca; Romania.

Honorary Mentions:

Simona Chişmore

Universitatea "Aurel Vlaicu", din Arad

Ionela Marinela Rotar

Universitatea "Aurel Vlaicu", din Arad

Maria Chifor

Universitatea "Aurel Vlaicu", din Arad

-Poster presentation

1st Prize: Ştefania-Adelina Milea

"Dunărea de Jos" University of Galati, Romania

2nd Prize: Nina-Nicoleta Condurache

"Dunărea de Jos" University of Galati, Romania

3rd Prize: Mioara Gabriela Slavu (Ursu)

"Dunărea de Jos" University of Galati, Romania.

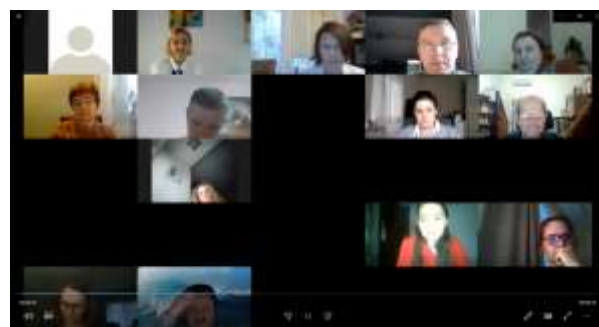
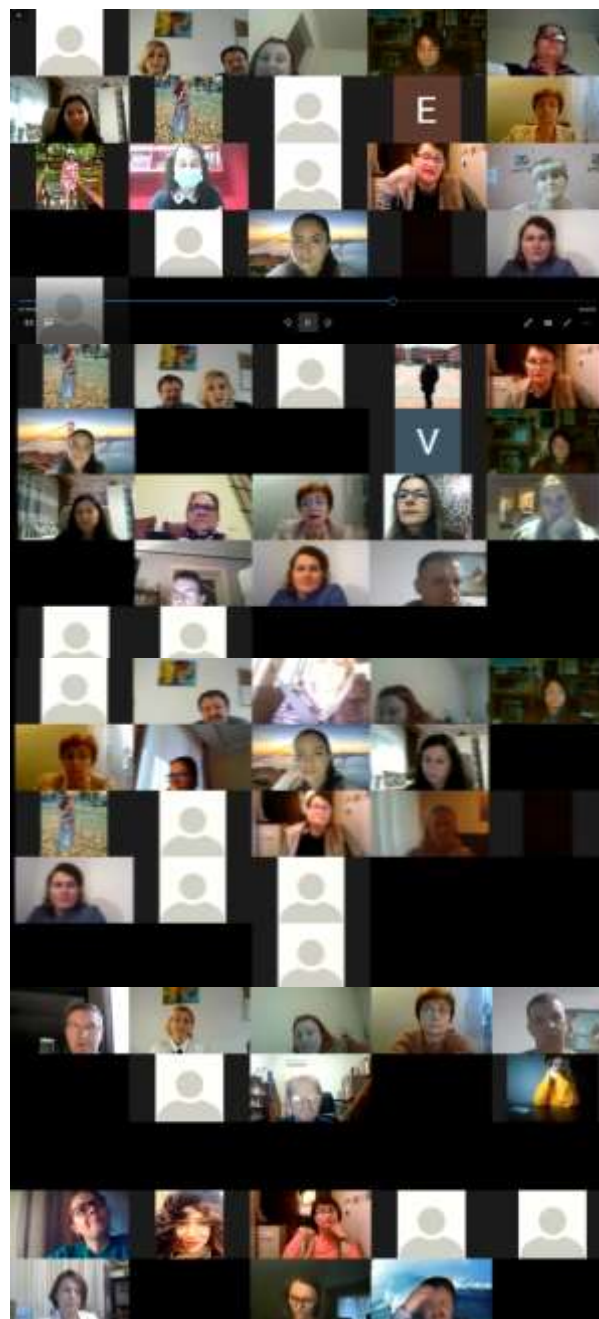
Mentiune: Purda Denisa-Emilia, Şerpescu

Patricia Florentina, Daniela Diaconescu

"Aurel Vlaicu" University of Arad, Romania.

The judges of the second session, which evaluated the presentations, were: Prof. Dr. Habil. Dana Copolovici, Assoc. Prof. dr. Dana Radu, Assoc. Prof. dr. Daniela Diaconescu, and Lecturer dr. Claudiu Ursachi from "Aurel Vlaicu" University.

The award ceremony was the best way to close the event, and the judges gave to each session: 1st, 2nd, 3rd prizes and Honorable Mentions, to recognize the work/results and to motivate further the participants to become good professionals in their domain.



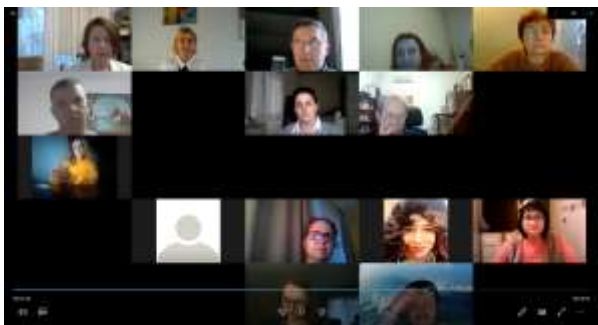


Fig. 2. Presentations held at The 18th Edition of the Student Scientific Session at Faculty of Food Engineering, Tourism and Environmental Protection, November 26th -27th 2020, on-line.

Due to current social problems, such as COVID-19 pandemic, climate changes, we believe that the future scientific events will continue to be held in virtual and/or hybrid formats. We agree that there are differences between in-person interaction and digitally-based interaction, and for students' events (symposiums, conferences, workshops, etc.) is very important that the hybrid/on-line formats will be emphasized in the future. In this way the scientific events will have more participants and the international participation will begin/increase in the near future, which is the main goal of our Students Scientific Session from "Aurel Vlaicu" University of Arad, Romania.

ACKNOWLEDGEMENTS

The author wants to thank to Ministry Of National Education from Romania, all members of the Organizing Committee, and our sponsors (SC SYKES ENTERPRISES EASTERN EUROPE SRL, SYKES, and Institute for Research, Development and

Innovation in Technical and Natural Sciences). We also thank to all the participants for their presentations and fruitful discussions.

REFERENCES

- Hoogendoorn, S., and Aye, Y., 2020, Empowering Global Chemical Biology at the Dawn of the New Decade: *Acs Chemical Biology*, v. 15, p. 1287-1291.
- Kindstedt, P. S., 2019, Symposium review: The Mozzarella/pasta filata years: A tribute to David M. Barbano: *Journal of Dairy Science*, v. 102, p. 10670-10676.
- Olena, A., 2020, COVID-19 Ushers in the Future of Conferences: *The Scientist*, v. Sep 28, p. 1-7.
- Woolston, C., 2020, Learning to love virtual conferences in the coronavirus era: *Nature*, v. 582, p. 135-136.



Open Access

This article is licensed under a Creative Commons Attribution 4.0 International License, which permits use, sharing, adaptation, distribution and reproduction in any medium or format, as long as you give appropriate credit to the original author(s) and the source, provide a link to the Creative Commons license, and indicate if changes were made. The images or other third party material in this article are included in the article's Creative Commons license, unless indicated otherwise in a credit line to the material. If material is not included in the article's Creative Commons license and your intended use is not permitted by statutory regulation or exceeds the permitted use, you will need to obtain permission directly from the copyright holder.

To view a copy of this license, visit <http://creativecommons.org/licenses/by/4.0/>.



ISSN 1582-1021

e-ISSN 2668-4764

**Edited by "AUREL VLAICU" University
Arad, Romania, 2020**